ADDIS ABABA UNIVERSITY
SCHOOL OF GRADUATE STUDIES

GROUNDWATER INVESTIGATION BY THE ELECTRICAL RESISTIVITY METHOD IN EL-GOF, MOYALE

SOLOMON HAILU

JUNE, 1997

GROUNDWATER INVESTIGATION BY THE ELECTRICAL RESISTIVITY METHOD IN EL-GOF, MOYALE

A Thesis
presented to
School of Graduate Studies Of
Addis Ababa University

In partial Fulfillment of
The Requirements For the Degree
Master of Science In Geophysics

By

Solomon Hailu Kebede

June 5, 1997

ACKNOWLEDGEMENT

I would like to express my deepest indebtedness to my advisor Dr. Tigistu Haile and Ato Shimelis Fisseha for the enormous help rendered to me in organising this project. I am deeply grateful to Prof. Roberto Balia for not only rendering his best help and co-operation but also providing me all the necessary materials for data processing.

I would be failing in my duty if I do not acknowledge my deep gratitude to all staff of the Geophysics Department, Ministry of Mines and Energy for their co-operation in making available to me their computer facilities and for their untiring assistance in organising this project

I extend my thanks to Dr. Tilahun Mammo for providing all sided assistance during the preparation and compilation of this paper.

TABLE OF CONTENTS

CONTENT (Continued)

CONTENT (Continued)

LIST OF FIGURE

Abstract

This paper describes the Resistivity Survey carried out in El-Gof area located some 38 km north of Moyale town in the Southern Borena region to locate and delineate a buried river channel which are of utmost importance in the siting of high yielding, more successful boreholes and in better understanding of the hydrogeology of buried valley aquifers.

Sixteen resistivity soundings using the schlumberger array with maximum AB/2 spread of 330 m were carried out. along three profile lines each 1 km long at an average line spacing of 200 m, and a VES interval of 150 m along the profiles.

All the field data were corrected for the effect of the first distance of MN spacing on resistivity values and then interpreted by using curve matching and an automatic iterative computer software program "SEV". During the interpretation process information from borehole data were also used and were found to be quite useful to refine the interpretation results.

Based on the results of the model interpretations of the sounding curves and from the measured apparent resistivity value, the respective geoelectric and pseudo-section of the area were constructed. The results obtained from these sections indicate on the average about five geoelectrical layers and areas of low and high resistivity values.

The low resistivity structures outlined at discrete locations in the NE and SW part are interpreted as the buried channel and the zone of high resistivity in the NW and SE part of the area correspond to shallow depth to the bed rock.

The buried channel is characterized by undulations with shallower and deeper sections. The deeper part of the buried channel is found in the SW part of the survey area which are likely to contain thick succession of sand and gravel deposits. These low resistivity areas were therefore chosen for water well drilling (borehole).

1. INTRODUCTION

1.1 BACKGROUND

Geophysical exploration methods are a primary tool for the investigation of the subsurface and are applicable to a very wide range of problems. Among the various techniques of geophysical prospecting, the electrical methods have branched out from a broader and more basic discipline - **Geoelectricity**, which utilizes the electrical properties of rocks, constitutes a very easy procedure for obtaining subsurface information from surface measurements.

The main property concerning the application of electrical methods is the ability of rocks to conduct an electric current (thier conductivity). The electrical conductivity of Earth materials can be studied by measuring the electrical potential distribution produced at the Earth's surface by an electric current that is passed through the Earth. Thus, the ultimate goal in electrical exploration is to make use of principles of geoelectricity and obtain geological maps of concealed structures, prospect for ores, minerals and oil, and solve many hydrogeological and engineering problems.

The electrical methods of exploration consist of various principles and techniques and make use of stationary as well as variable currents produced artificially or by natural ways. Among these diverse techniques, the one most extensively used in prospecting for groundwater and the one with which this paper is mainly concerned is known as the **electrical resistivity** method. In this method, a direct current or a low frequency alternating current is introduced into the ground using a pair of electrodes and the resulting distribution of the potential in the ground is measured by using another pair of electrodes connected to a sensitive voltmeter.

The variation of resistivity with depth is studied by a progressive increase of current electrode separation so that the effects of rocks at depth will be more significant. This method is known as **vertical electrical sounding.(VES)** Lateral resistivity variations are studied using the method of **horizontal profiling** for a fixed current and potential electrode separations along a traverse line. The resistivity value is determined from the relation developed using potential drop, measured current and the geometrical configuration of the electrodes. If the ground is homogenous the resistivity calculated will be independent of electrode spacing and location. But in reality, since the ground is locally inhomogenous the resistivity varies with the relative position of electrodes. The subsurface rock resistivity variation affects or perturb the electrical current flow lines and these in turn affect the distribution of surface electrical potential lines, compared to their pattern over a homogenous medium. The quantity then computed is known as the **apparent resistivity** (ρ_a). Therefore, from the measurement of potentials / potential gradients on the surface, it is possible to know something about the nature of the subsurface layers.

The electrical resistivity methods have been successfully applied in the study of different geological and hydrogeological problems. Particularly in hydrogeology, it is the most extensively used geophysical techniques, being routinely and widely employed in groundwater exploration to locate zones of relatively high conductivity corresponding to water saturated strata. In addition, the methods provide with structural and lithological information such as, the location of fault and shear zones which could affect the pattern of ground water flow, the location of ground water table, etc. Thus, the method provides an adequate depth penetration and quantitative results without the large cost involved in an extensive drilling program (Kearey et al., 1984).

The usefulness of the resistivity method in solving geological and hydrogeological problems depends, to a considerable extent, on the subsurface resistivity contrast. In considering the resistivities of various geologic units it is found that the overall resistivity is very sensitive to variation in porosity, water content, and water quality (ionic concentration) and can be considerably lower than the resistivity of the rock matrix.

The electrical resistivity methods (both Sounding and Profiling) have been applied for successful mapping of buried river valleys and for ground water investigation in different countries (Emilia et al., 1976; Van Overmeeren, 1981; Bezerra, 1979; Cavalcanti, 1979; Kobayashi, 1979; Parsoni, 1981; Getenet Mewa et al., 1996; Kramvis, 1987). However, the effectiveness of the method should be studied adequately over the relevant geological structures and under the actual field conditions.

In the southern Borena region, where the climate is semi-arid to arid, and the major rock types are of Precambrian basement complex, locating reliable and dependable groundwater resources is a difficult task in such an environment. Most commonly, in such an area, the search for groundwater starts with an investigation of unconsolidated sediments. It has been reported in hydrogeological studies conducted in the area (Bekele Dewano et al., 1988; Tesfaye Chernet, 1993) that unconsolidated deposits of high groundwater resource potential exist located mainly on a narrow and long ancient river channel.

In fact, modern drainage follows the old drainage, and generally flows from West to East in a very large area in broad flat channels within undulating landscapes. The major channels follow an East-West trend and have a latitudinal preference at about 3°50′ N and 4°30′ N.

Buried river channels usually contain sand and/or gravel which are good aquifers, and some of the highly yielding aquifers have been found on the deposit covering the plains of

El-Gof and El-Leh. The main aquifer in the area is transported sediments of sand and gravel overlain by lake deposits. However, as the buried channels have no surface expression, techniques that would assist to locate and delineate them are of utmost importance in the siting of high yielding, more successful boreholes and also in better understanding of the hydrogeology of buried valley aquifers.

It has been found that the electrical resistivity method works best in areas having contrasting lithological resistivity. This favorable condition exists in the area of interest due to the significant resistivity/conductivity difference between the low resistivity unconsolidated sediments and the underling more compact and dense bedrock.

Based on this suitable condition and the past geological and hydrogeological information, it was decided to conduct an electrical resistivity survey (sounding) in El-Gof to locates possible areas of groundwater exploitation and best sites for location of boreholes.

1.1.1 OBJECTIVES

The main objectives of the resistivity survey were :

. delineating the extent and trend of the buried river channel;

. evaluating the usefulness of the method in such geologic situations;

. delineating probable zones of water saturation (aquifers) within the sedimentary section

. comparing the findings of the resistivity survey with the results of the previous gravity survey carried over the same area.

The electrical resistivity method with the vertical electrical sounding variation was employed to achieve these objectives. The electrode configuration used was the Shlumberger

1.2 THE SURVEY AREA

1.2.1 LOCATION AND ACCESSIBILITY

The survey area, El-Gof, is situated in Southern Ethiopia, some 38 km North of Moyale town. Moyale, on the Ethio-Kenyan border is 775 km South of Addis Ababa, and is connected by asphalted road with it. A dry weather road connects El-Gof with Moyale (Fig. 1). The geographic coordinates (latitude/longitude) of El-Gof are about 3°51′ N and 39° 04′ E, respectively.

The survey area has a flat topography with an average altitude of about 1140m above sea level and falls within the Lega Sure Basin which drains the large plain north of Moyale through an indefinite network into Kenya.

The rainfall pattern is bimodal with periods of long and short rains stretching from March through May and September through October, respectively. The mean annual rainfall is in the range of 400-500 mm (Coppock, 1994).

1.2.2 PREVIOUS GEOPHYSICAL WORKS

Recently, Mogas Tigabe (1996) has carried out gravity survey over the area and has found that the buried channel has a meandering pattern with a high degree of sinuosity and also exhibits undulations (shallow and deep) along its course. He has also located the most favorable site for borehole drilling. However, no other geophysical methods have been conducted in the study area to confirm his findings.

1.2.4 GEOLOGY AND HYDROGEOLOGY OF THE SURVEY AREA

The major geological formations in the Borena region as described in Coppock (1994) are presented in simplified form in Fig. 1. The map shows that the area is underlain by various rock types ranging in age from recent to pre-Cambrian which are described as follows:

Pre-Cambrian Basement Complex

This comprises about 38% of the study area, and consist of granites, gneiss and migmatites. The areas covered by the basement complex largely run from Northwest to South-east from Yabelo to Moyale and Northeast of Arero. Small circular and elongated patches of the basement complex occur in the central part often as peaks because of their resistance to erosion.

Sedimentary Deposits

These were deposited during the Jurassic period some 180 million years ago. They comprise about 2% of the area, to the North-East and are composed of shale, sandstone and limestone.

Volcanics

These comprise about 20% of the area and were formed during the Tertiary and Quaternary periods. Volcanics consist of a trap series component to the West, fissoral basalts to the Southwest and quaternary basalts to the South. All of these overlie the basement complex formations and reach up to a thickness of 500m.

Quaternary Deposits

These comprise about 40% of the area. They have resulted from alluvial, lacustrine and elluvial processes, and are common in valleys and depressions.

The survey area lies in what is mapped in Fig.1 as quaternary deposits. Of these elluvial and lacustrine sediments are the major ones and occur along a broad and flat channel. The presence of a buried river channel has been reported earlier although its exact location and character is not precisely known. It may be hypothesized that during the quaternary climatic changes in favor of wet periods coupled with structural disturbances of the basement resulted in erosion along structurally weak zones which ultimately developed deep channels into which superficial sediments were deposited.

It was not well understood whether the alluvial or lacustrine sediments form the main aquifer in the area. Some of the previous hydrogeological investigations (Bekele Dewano et al., 1980; Tesfaye Cherinet, 1993) reported the lacustrine sediments to have high groundwater resource potential. But others (Zenaw Tessema and Meles Belachew, personal communication) have recently proven that the alluvial sediments constitute a good aquifer with the lacustrine sediments acting only as confining layers.

Four boreholes, labeled as BH1-BH4, exist in the survey area. Boreholes BH1 and BH2 were drilled by the Water Supply and Sewerage Authority (WSSA) in 1988 and these boreholes are meant to supply Moyale town. Borehole BH3 was drilled by an Italian NGO, LVIA, in 1995 and is equipped with motorized pump, whereas, BH4, with hand pump, was drilled in 1994 by the Oromia Bureau for Natural Resources Development and Environmental Protection (ONRDEP). Both boreholes supply water for the local community, as described by (Mogas Tigeba, 1996).

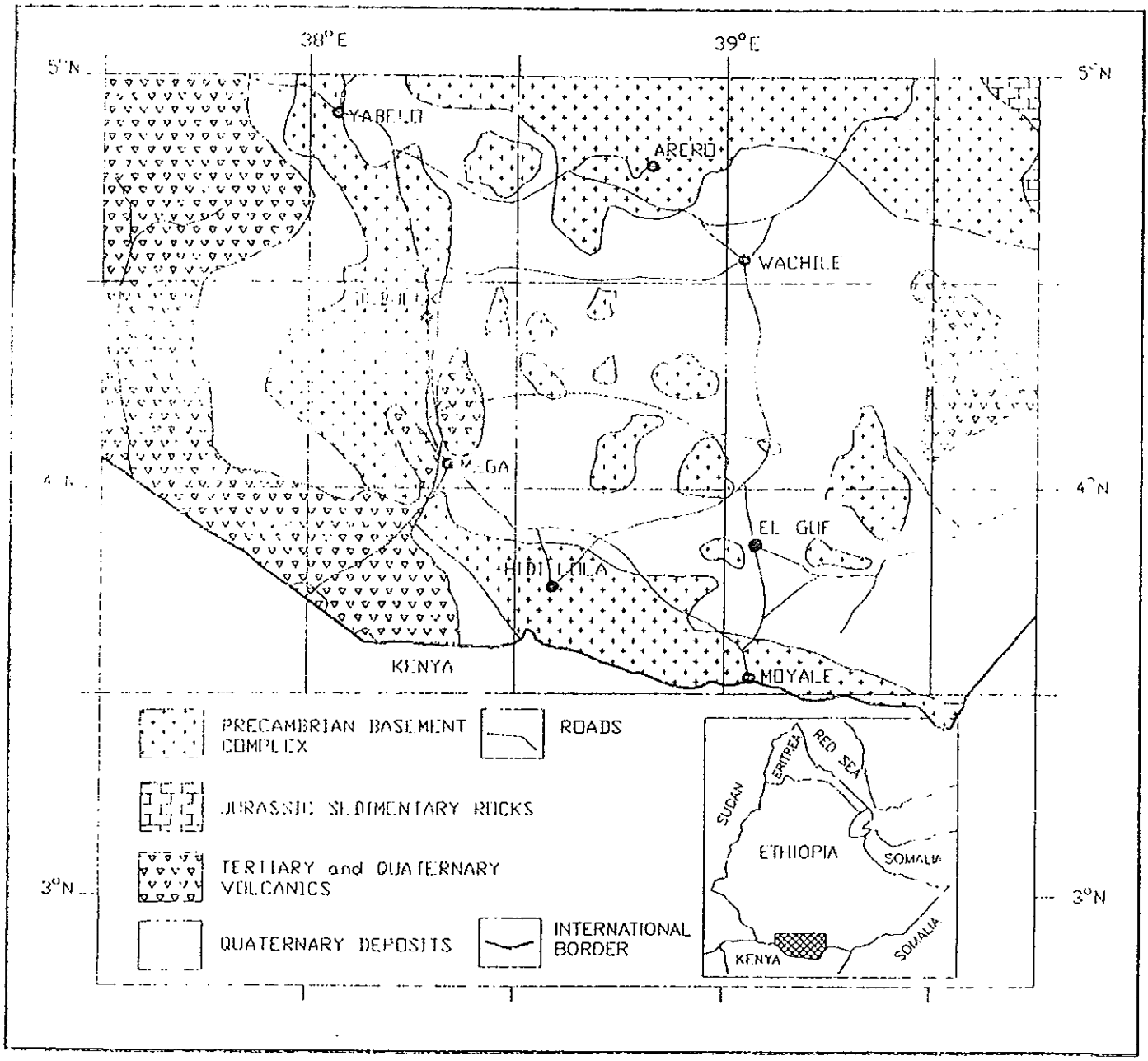

FIGURE 1. REGIONAL GEOLOGY AND LOCATION OF THE STUDY AREA

According to the available geological log of BH4, the underlying lithounits comprises the following:

ONRDEP well log

Depth (m)	Lithology
0.0 - 1.5	Slity clay
1.5 - 9.0	Marly
9.0 - 21.0	Sandy limestone
21.0 - 33.0	Sandy gravel
33.0 - 42.0	Gravely sand
42.0 - 50.0	Biotite schist

In addition to the above boreholes, another borehole exists about 75 m Northeast of the survey area and it was drilled by the Ministry of Mines. But this borehole is not presently functional.

The geologic log data for this well are given below:

Depth (m)	Lithology
0.0 - 0.5	Clay
0.5 - 10.0	Marly limestone
18.0 - 26.0	Medium sand
26.0 - 39.0	Coarse sand
39.0 - 42.0	Weathered schist
42.0 - 48.9	Fresh schist

2 . MATHEMATICAL FOUNDATIONS AND SURVEYING PROCEDURE

2.1 FUNDAMENTALS OF DIRECT CURRENT FLOW IN HOMOGENEOUS EARTH

The fundamental principles of direct current flow in homogenous earth was discussed in detail (Telford et al., 1976; Parasnis, 1962; Dobrin, 1976; Hummel, 1932; Keller and Frischknecht, 1966; Koefoed, 1979; etc.). The brief description of the principles are presented as follows:

The flow of current in a medium is based on the principle of conservation of charge, mathematically this principle is expressed as

$$\text{div } J = \partial q/\partial t \qquad (2.1)$$

where J is current density

q is the charge density

Since stationary electric field is conservative and is a function of a scalar potential V, one get

$$E = -\nabla V = -\text{ grad } V \qquad (2.2)$$

Ohm's law relates the current density J and the electric field intensity E by

$$J = \sigma E = 1/\rho E \qquad (2.3)$$

Substituting eqn. (2.2) in eqn. (2.3) gives

$$J = -1/\rho \nabla V = -\sigma \nabla V \qquad (2.4)$$

where ρ is the resistivity of the medium

σ is the conductivity of the medium ,and

V is the electric potential

For an isotropic medium the resistivity/conductivity is a scalar function of the point of observation and J is in the same direction as E but for an anisotropic medium resistivity or conductivity is a second rank tensor and J will assume a directive property and may not always be in the direction of E.

For stationary/direct current

$$\partial q/\partial t = 0$$

and eqn. (2.1) reduces to the form

$$\text{div } J = 0 \qquad (2.5)$$

Substituting eqn. (2.4) in eqn. (2.5) we have

$$\text{div } [\sigma \nabla V] = \text{div } [1/\rho \nabla V] = 0$$

or expanding, we get

$$\text{grad } 1/\rho \text{ grad } V + 1/\rho \text{ [div grad V]} = 0 \qquad (2.6)$$

This is the fundamental equation of electrical prospecting with direct current flow. If the medium is homogeneous, ρ is independent of the coordinate axes and the above equation reduces to

$$\text{div (grad V)}$$

or $$\nabla^2 V = 0 \qquad (2.7)$$

Thus the electric potential distribution for direct current flow in a homogeneous isotropic medium satisfies **Laplace's Equation.** Next we shall consider how the resistivity is related to practically measured potential (or potential difference) when current I is introduced into the ground.

2.2 POTENTIAL DISTRIBUTION DUE TO A CURRENT SOURCE

Case (i) : **A point source of current over an infinite homogeneous medium**

Considering an infinite conducting layer of uniform resistivity (ρ) and a current of strength I entering at point C_1 with a single current electrodes (Fig.2)

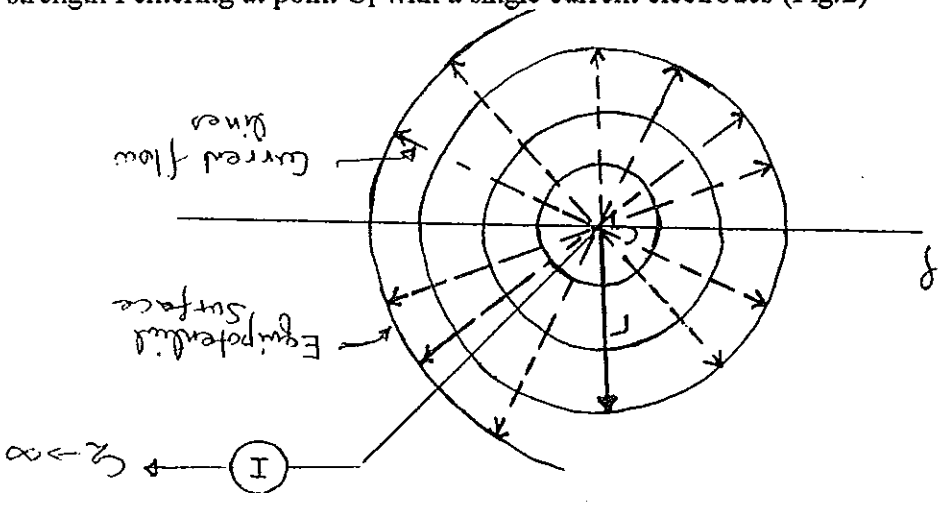

Fig.2 : Infinite conducting layer

The current circuit is completed through another electrode placed at far distance away that its influence is negligible. Because of the symmetry for this case the potential at a distance r from the point of introduction of the current, C_1, will be only a function of r, and Laplace's equation reduces to

$$\nabla^2 V = d^2V/dr^2 + 2/r\ dV/dr \qquad (2.8)$$

multiplying by r_2 and integrating eqn. (2.8) from r to infinity we get the solution as

$$V_r = A/r + B \qquad (2.9)$$

where A and B are integration constants

From the boundary condition that the potential V at infinite distance ($r \to \infty$) is zero gives B = 0. For this case, the equipotential surfaces given by V = A/r = constant or r = Constant, are clearly seen to be spherical; and the electric field lines and current lines, as well as being the gradient of the potential, point in the radial direction as shown in Fig.2.

The current density J at a distance r is given by

$$J = -\frac{1}{\rho}\frac{dV}{dr} = -\frac{1}{\rho}\frac{d}{dr}\left(\frac{A}{r}\right) = \frac{1}{\rho}\frac{A}{r} \qquad (2.10)$$

The total current flowing out of a spherical surface of radius r (of surface area = $4\pi r^2$J) is given by

$$I = J \times 4\pi r = 4\pi r \left(\frac{1}{\rho}\frac{A}{r}\right) \qquad (2.11)$$

But this total current is equal to the original current I, introduced at point C_1.

$$I = \frac{4\pi A}{\rho} \quad \Rightarrow \quad A = \frac{I\rho}{4\pi}$$

then frome eqn. (2.9)) and the fact that B=0,

$$V = \frac{I\rho}{4\pi r} \qquad (2.12)$$

Eqn. (2.12) is the basic equation of the electrical resistivity method to determine the resistivity of an infinite homogeneous earth which can be given by

$$\rho = 4\pi r \frac{V}{I}$$

or $\rho = 4\pi R$ (2.13)

where R is earth resistance

Case (ii) : <u>A point source of current 0vern a semi-infinite homogeneous medium</u>

Consider a semi-infinite homogeneous and isotropic medium with a single current electrode on the surface, Fig. 3, the current distribution is radialy outward and uniform over a hemispherical shell developed bv connective hemispheres of equipotential surfaces

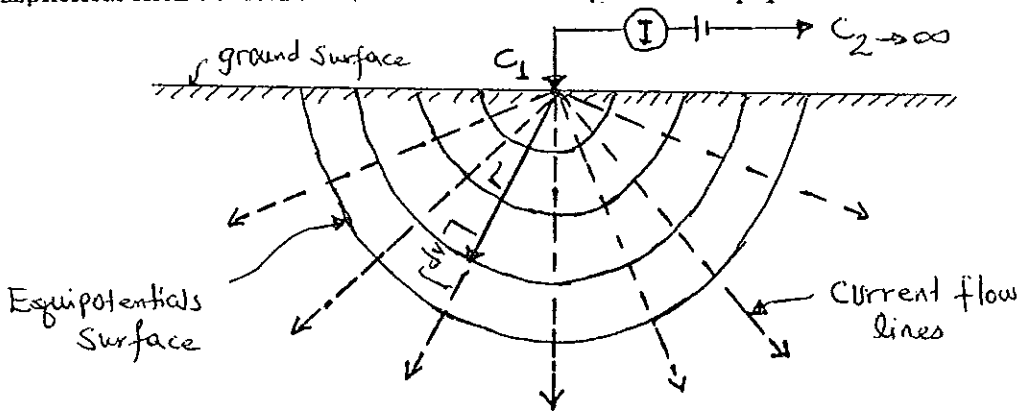

Fig. 3 : Distribution of current in a semi-infinite medium due to a point source of current

For a semi-infinite homogeneous and isotropic medium all other conditions in case (i) remaining unchanged but in this case the current distribution is radially outward and uniform over a hemispherical shell developed by connective hemispheres of equipotential surfaces as shown in Fig. 3.

The current density J at a distance r from a current source is given by:

$$J = -1/\rho dV/dr = -1/\rho A/r^2 \quad (2.14)$$

Then the total current flowing out of a hemispherical surface of radius r (surface area $2\pi r^2$) is given

$$I = 2\pi r^2 J = 2\pi r^2 \left(\frac{A}{\rho r^2}\right)$$

$$\Rightarrow \quad A = I\rho/2\pi$$

Hence, the potential at any point due to a single current source at the surface of a homogenous earth becomes

$$V = \frac{I\rho}{2\pi} \frac{1}{r} \tag{2.15}$$

Thus, in this case

$$\rho = 2\pi r \frac{V}{I} \tag{2.16}$$

Case (iii) : <u>Two sources of current over a semi-infinite medium</u>

If one considers a finite distance between the two current electrodes (the source and the sink) as shown in Fig. 4, the potential at any nearby surface point will be the sum of the potential contribution made from booth electrodes.

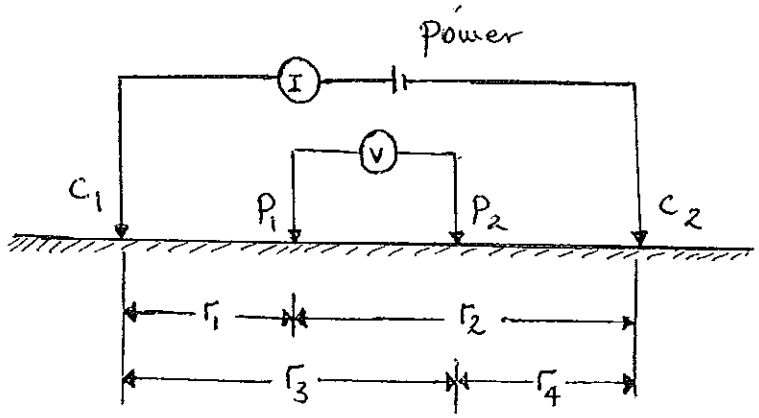

Fig. 4 : Potential distribution and current flow from two surface electrode arranged in generalized linear form

From equ. (2.16) the potential at point P_1 is given by

$$V_{c1} = \frac{I}{2}\frac{\rho}{\pi}\left(\frac{1}{r_1}\right)$$

(ii) Due to sink (C_2)

$$V_{c2} = -\frac{I}{2}\frac{\rho}{\pi}\left(\frac{1}{r_2}\right)$$

Conventionally the source gives rise to a positive potential and the sink gives rise to a negative potential. Thus, the resultant potential at P_1 is given by

$$V_{p_1} = V_{c1} + V_{c2} = \frac{I}{2}\frac{\rho}{\pi}\left[\frac{1}{r_1} - \frac{1}{r_2}\right] \qquad (2.17)$$

Similarly the total potential at point P_2 will be

$$V_{p_2} = \frac{I}{2}\frac{\rho}{\pi}\left[\frac{1}{r_3} - \frac{1}{r_4}\right]$$

Then, for a current of intensity I entering through C_1 and coming out through C_2 the potential difference ΔV, in between the inner potential electrodes P_1 and P_2 will be ,

$$\Delta V = V_{p_1} - V_{p_2} = \frac{I}{2}\frac{\rho}{\pi}\left[\left(\frac{1}{r_1} - \frac{1}{r_2}\right) - \left(\frac{1}{r_3} - \frac{1}{r_4}\right)\right]$$

or $$\Delta V = \frac{I}{2}\frac{\rho}{\pi}\left[\frac{1}{r_1} - \frac{1}{r_2} - \frac{1}{r_3} - \frac{1}{r_4}\right] \qquad (2.19)$$

Therefore,

$$\rho = 2\pi(\Delta V / I)K \qquad (2.20)$$

where $K = \left[\frac{1}{r_1} - \frac{1}{r_2} - \frac{1}{r_3} + \frac{1}{r_4}\right]^{-1}$ is a characteristic of the electrode arrangement used,

and is called the **Geometric Factor** of an electrode configuration.

2.2.1 CONCEPT OF APPARENT RESISTIVITY

In the interpretation of direct current (DC) potential field measurement the notion of "**Apparent Rresistivity**" is frequently used. If the ground was electrically homogenous, a single measurement of the potential difference and of the current would determine its resistivity. Therefore, the resistivity calculated from eqn. (2.20) would be constant and independent of the electrode spacing and location for a homogeneous earth. But, for an inhomogeneous earth, resistivity varies and the computed value from eqn. (2.20) is called the **apparent resistivity**, the resistivity which the ground would have if it was homogeneous. Thus, the apparent resistivity of a geologic formation medium depends upon the geometry and the resistivity of the various elements conststutig the given formation. and the expression for the apparent resistivity can be written as,

$$\rho_a = K\,\Delta V/I$$

To illustrate this concept, consider the case of a layer having a thickness h and resistivity ρ_1 overlying a second homogeneous and isotropic layer of infinite thickness and of resistivity ρ_2 where $\rho_2 - \rho_1$ is high. In this case the current will no longer flow along approximately circular arc as it did in homogeneous earth. Rather ,the lines of flow pattern will be distorted as shown in Fig. (5), because the lower resistivity below the interface result in an easier path for the current within the deeper zone. If the current flow is distorted in passing from a medium of one resistivity into another, the equipotential also distorted.

It is evident that, as the distance between electrodes C_1 and C_2 is changed, the value of ρ changes and can be calculated (eqn2.19 Specifically, when the distance $C_1 - C_2$ is small with

respect to h, the thickness of the first layer, the resistivity approximates ρ_1 of this layer. However, if the distance C_1 - C_2 is very large with respect to h the resistivity approaches ρ_2. The value of ρ in the intermediate case is comprised of ρ_1 and ρ_2. Thus we call ρ the apparent resistivity.

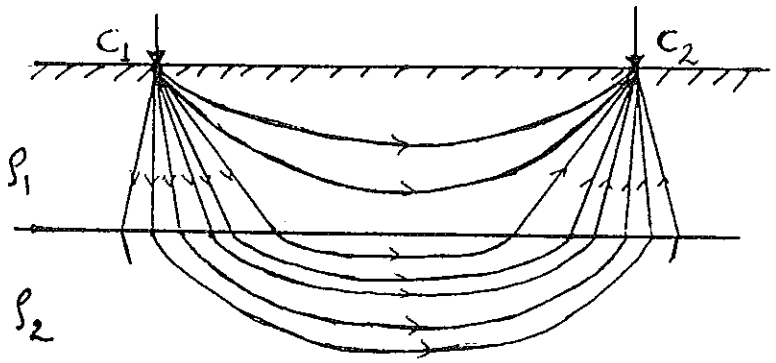

Fig. 5 : Lines of current flow between current source C_1 and C_2 in two layered earth

Therefore, eqn. (2.20) provides the basic expression for calculating apparent resistivity for any well known electrode configuration and if the configuration are laid down over the layered earth then the resistivity result by any of the configuration is called the apparent resistivity.

2.2.2 POTENTIAL DISTRIBUTION AT THE SURFACE OF A HORIZONTALLY STRATIFIED EARTH.

In section (2.2), the general distribution of potentials in homogeneous and isotropic medium has been discussed. This section summarizes the potential due to a layered uniform earth and its relation to the layer parameters. There are a number of mathematical approaches which have been used in calculating potential fields in a layered media.

A. The two layer problem

The simplest configuration for which theoretical solutions can be generated is the two layered earth shown in Fig. (6).

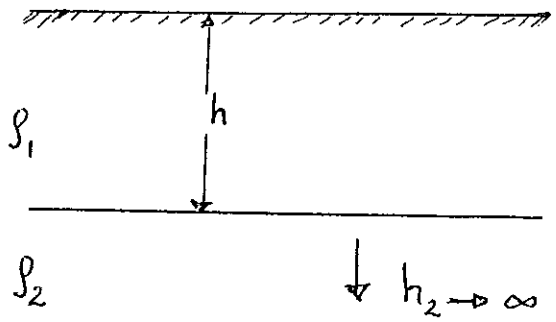

Fig. 6: Two layered earth

There is one superficial strata with a resistivity ρ_1 and thickness h overlying a second strata of resistivity ρ_2 and infinite thickness.

Two methods the image and Laplace solution methods have been developed to calculate the potential field in a layered medium. The simplest approach to this problem is the method of images.

Method of Images: The image solution was first proposed by Hummel (1932) and improved by a number of workers, Cagniard (1952); Koefoed (1960); Homilius (1961), and Orellana and Mooney (1966). The method is based on the analogy between the mode of current flow through the earth and the path taken by light rays in passing through optically different mediums in which case the electric current density and the light intensity decreases as the square of the distance from the origin increases. The method involves a

single overburden of layers where the potential distribution due to a point source is determined in a medium separated from another adjacent medium by a plane boundary.

The intensity of the fictious current decreases by a factor of k, called **Reflection Coefficient.**

$$\text{If } \rho_2 \to \infty, K = \frac{1 - \frac{\rho_1}{\rho_2}}{1 + \frac{\rho_1}{\rho_2}} = 1$$

$$\text{If } \rho_2 \to \infty, K = \frac{\frac{\rho_2}{\rho_1} - 1}{\frac{\rho_2}{\rho_1} + 1} = -1$$

Thus the value of the reflection coefficient lies between +1 and -1 depending on the relative resistivities in the two media.

As k for air is 1, the intensity of each successive unique source is reduced by the reflection coefficient (k) between the layer boundaries, the intensity of the image is given as

$$I^n = k^n I$$

Hence, the potential at a point on the surface is given by the sum of the potential due to a source at the surface and an infinite series of image sources or fictitious origins. Thus, the resultant potential at any point on the surface can thus be expressed as an infinite series of the form

$$V_p = \frac{I \rho_1}{2\pi}\left[\frac{1}{r} + \frac{2K}{r_1} + \frac{2K^2}{r_2} + \ldots + \frac{2K^n}{r_n} + \ldots\right]$$

where $r_n = \sqrt{r^2 + (2nh)^2}$ n = 1, 2, 3, ...

This series can be written in the compact form as :

$$V(r) = \frac{I\rho_1}{2\pi}\left[1 + 2\sum_{n=1}^{n=\infty} \frac{K^n}{\sqrt{1+\left(\frac{2nh}{r}\right)^2}}\right] \qquad (2.21)$$

where, r is the distance from the current source to the measuring point.

In this series the first term is the potential function for a homogeneous isotropic half-space called primary or normal potential, and the second term is called a disturbing potential. This basic formula is extended to provide the potential distribution due to a four electrode system where, at any potential electrode a potential due to two current source is determined using eqn. (2.19).

For two layer earth, the apparent resistivity expression for any four electrode system is developed from the potential field equation eqn.(2.21) using the potential field formulas for any array. The mathematical derivations are found in a number of geophysical books, namely: Telford et al., (1976), Keller and Frischknecht (1966) etc.

B. The N-Layer problem

This problem can be solved by finding the solution of the Laplace equation that satisfies a certain boundary condition. In solving the Laplace equation the method of separation of variables or Hankel transform method are used.

The main assumptions to the solution of the potential field are:

1. The subsurface consists of a finite number of layers separated from each other by horizontal boundary planes, the deepest layer extends to infinite depth, the other layers have finite thickness.
2. Each of the layers is electrically homogeneous as well as electrically isotropic and the field is generated by a point source of direct current that is located at the surface of the earth.

The expression for the potential field in the condition specified above has been derived by Stefanescu and Schlumberger (1930), and involves the determination of the potential at a point with respect to the resistivity of the upper most layer ρ_1 and at distance r from a current source of strength I. It is defined by

$$V(r) = \frac{I\rho_1}{2\pi r}[1 + 2\int_0^{\infty} K(\lambda) J_0(\lambda r) d\lambda] \qquad (2.22)$$

where, V is the potential at a point on the surface

λ is a variable of interpolation

J_0 is Bessel function of zero order

$K(\lambda)$ is Slichter kernel function.

K is controlled by the thickness and resistivities of the underlying layers.

The recurrence relations given by Pekeris (1940) and Flathe (1955) can be used to determine Slichter's kernel function. Flathe's recurrence relation describes the addition of a new layer at the bottom of the layer sequence where as the Pekeris recurrence relation describes the addition of a new layer at the top of the layer sequence, combined with the displacement of the electrode configuration to the top of the newly added layer. Both the Flathe and Pekeris recurrence relations have their own specific field of operation. However, in some applications either one may be used, in such a cases Pekeris' is preferred because of its simpler structure and the consequent economy in the computer memory space.

The Pekeris recurrence relation is given as (Koefoed, 1979).

$$K_i = \frac{[K_{i+1} + q_i \tanh(\lambda t_i)]}{[q_i + k_{i+1} \tanh(\lambda t_i)]} \qquad (2.23)$$

This can be used to determine Slichter's kernel function in the surface layer when the parameters of the layer distribution are known.

Applying the boundary conditions one can get K_n=1, for the substratum (that is, n^{th} layer). Then using the value of K_n one can find the value of K in any other layers by recurrent application of eqn. 3.

Koefoed (1970) introduced the "**Resistivity Transform**" denoted by T(λ), which is defined by the equation

$$T_i = \rho_i K_i \tag{2.24}$$

The Pekeris recurrence relation, expressed for the resistivity transform are

$$T_i = \frac{[T_{i+1} + \rho_i \tanh(\lambda t_i)]}{[1 + T_{i+1} \tanh(\frac{\lambda t_i}{\rho_i})]} \tag{2.25}$$

Using eqn. 2.21 and eqn. 2.24 the potential due to a point source, is given as

$$V(r) = \frac{I}{2\pi} \int_0^\infty T(\lambda) J_0(\lambda r) d\lambda \tag{2.26}$$

where T(λ) is the resistivity transform

Eqn.2.26 may be written as a convolution integral by making the following change of variables, r = exp (x) and λ = exp (-y)

this is in order to have the same dimension for x and y as λ 's dimension is a reciprocal of length.

$$V(r) = \frac{I}{2\pi r} \int_{-\infty}^\infty T(y) \exp(x - y) J_0(\exp(x - y)) dy$$

$$V(r) = \frac{I}{2\pi r} \int_{-\infty}^\infty T(y) f(x - y) dy \tag{2.27}$$

Thus, the potential is given by the convolution of the transform function with a so-called filter function which has the form

$$f(x-y) = \exp(x-y)\, J_0(\exp(x-y))$$

This convolution may be expressed in discrete form as Rijo et al., (1977).

$$V(r) = \frac{I}{2\pi r} \sum_{j=n_1}^{j=n_2} T(Lnr - n_j) C(n_j) \qquad (2.28)$$

where, n_j are filter coefficient abscissa

$C(n_j)$ are the digital filter coefficients

n_1 is the number of coefficient to the left of the filter origin

n_2 is the number of coefficient to the right of the filter origin

The apparent resistivity for any configuration for a layered earth can be obtained using eqn. 2.28.

2.3 METHODS OF RESISTIVITY SURVING

2.3.1 ELECTRODE ARRANGEMENT

A direct current I is introduced in to the earth through two current electrodes C_1 and C_2 and the resulting potential difference between any two points on the surface can be measured by using another two potential electrode P_1 and P_2. Then using Eqn. (2.19) the potential difference for any electrode configuration can be found. In actual practice a number of different surface configurations are used for the current and potential electrodes. But, the most common arrangement are :

a) Symmetrical arrangement

b) Dipole arrangement

In the symmetrical arrangement, the electrodes are aligned on a straight line and the potential electrodes are symmetrically placed about the center of the straight line. Fig. 7 shows the Symmetrical array and Fig. 8, the generalized Dipole-Dipole array.

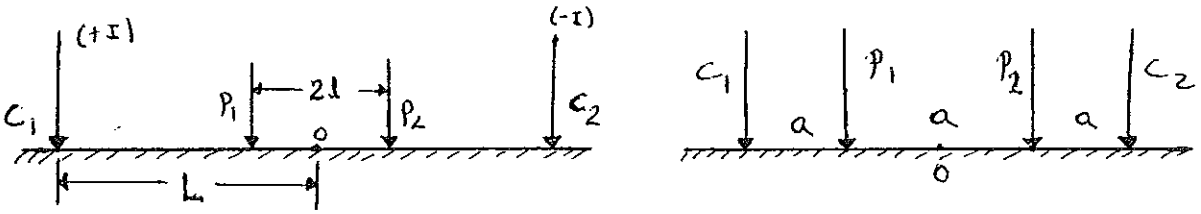

a)Schlumberger b)Wenner

Fig. 7 : Symmetrical array

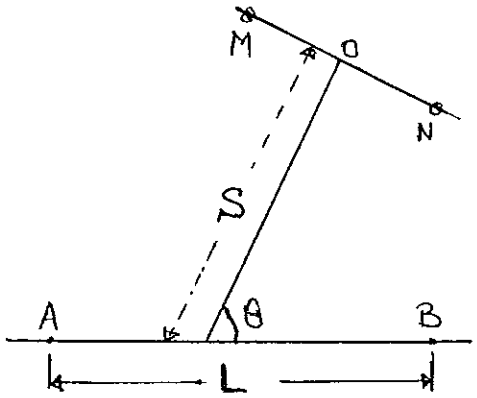

Fig. 8 : The General Dipole-Dipole configuration

A few of the various electrode configurations are discussed here with the aim that this will enable one to understand the special significance of each array and their limitations

a) <u>The Schlumberger configuration</u>:

In this arrangement the electrodes are symmetrically placed around a point Fig.(7a), so that,

$r_1 = L-l$, $r_2 = L+l$, $r_3 = L+l$ and $r_4 = L+l$

$$\Delta V = \frac{I}{2}\frac{\rho}{\pi}[1/(L-l)-1/(L+l)-1/(L+l)-1/(L+l)]$$

or $$\Delta V = \rho\frac{I}{\pi}[2l/(L^2-l^2)]$$

and from which the apparent resistivity is obtained as,

$$\rho_a = \frac{\pi}{2}(L^2-l^2)\frac{l}{I}\Delta V/l = K\Delta\frac{V}{I} \qquad (2.29)$$

where $K = \frac{\pi}{2l}(L^2-l^2)$ is the geometrical factor

The Schlumberger array has its l much less than L ($L \geq 5l$) and so one can approximate (L^2-l^2) by L^2 with an error less than 4% ;and in this case the apparent resistivity becomes

$$\rho_a = \frac{\pi}{2}\frac{L^2}{l}\Delta V/I = \frac{\pi}{2}\frac{L^2}{l}\Delta V/I = \frac{\pi}{2}L^2\frac{E}{I}$$

Hence ΔV is taken as $\Delta V/l$ which is a potential gradient. Because of this the Schlumberger arrangement is called a gradient arrangement.

The method involves measurement of a potential gradient and so potential electrodes are placed close enough so that the ratio of measured voltage to potential electrode separation approximately equals the voltage gradient at the mid point of the current electrode distance (2L). Thus, the apparent resistivities obtained are close to the average ground resistivity. The exact potential gradient can not be measured, since it represents the limit of the ratio of voltage to potential spacing as the electrodes move closer together. It is also because potential can not be measured in the limiting case of zero separation. The error introduced due to the finite distance of potential spread is evaluated by considering the geometric factor for which the gradient is measured (Keller and Frischknecht, 1966) so that

the apparent resistivity will be within a given error limit. It is necessary to limit the error to within a 5% ordinary error limit in the apparent resistivity measurements.

With the Schlumberger array the effects of local inhomogeneity which lie close to the potential electrodes, can be easily identified on the resistivity curve as compared to the Wenner array. This is because of the advantage in the Schlumberger array that the potential spread remains constant for a series of current electrodes, and the effect will be similar for a series of measurements. Hence, there will not be any appreciable change in the shape of the different segments of the resistivity curve, rather they are shifted by a constant factor. This condition enables one to make corrections so that the resistivity curve can be reconstructed as it would be obtained in a laterally homogeneous earth. In the case of the Wenner method the potential spread is displaced for each current electrode displacement and the effect of local inhomogeneties is an erratic apparent resistivity curve. However, techniques have been developed for the Wenner configuration which enable one to identify and quantify these inhomogeneity effects. Such techniques are the tripotential and offset-Wenner.

b) The Wenner configuration

The electrode configuration is given in Fig.7b. The current and the potential electrode spreads are kept equal, so in this case $r_1=a$, $r_2=2a$, $r_3=2a$ and $r_4=a$ and thus

$$\Delta V = \frac{I\rho}{2\pi}\left(\frac{1}{a}\right)$$

so that the apparent resistivity for Wenner configuration is expressed by,

$$\rho_{a_w} = 2\pi a \frac{\Delta V}{I} = K \frac{\Delta V}{I} \qquad (2.30)$$

where, ΔV is measured voltage

I is measured electric current and

K = 2πa is the geometric factor

and this configuration is known as a potential configuration (because of the presence of ΔV/I in the expression).

c) The Dipole -Dipole configuration

The general Dipole-Dipole configuration is indicated in Fig.8. The practical advantage of the Dipole-Dipole over the Wenner and Schlumberger arrays is that it requires shorter length of cable for a comparable depth of investigation. This condition provides the possibility that the distance between the current source and the voltage receiver positions can be increased almost indefinitely and measurable signals are recorded. It is mostly applied in induced polarization surveys to locate ore veins and also for deep investigations.

2.3.2 SURVEYING PROCEDURE

There are two basic field procedures used in an electrical resistivity survey:

a) Electrical sounding:

In which the center of the electrode spread is maintained at a fixed location, and the electrode spacing is increased.

In this procedure, also called the vertical electrical sounding (VES), the electrode configuration most commonly used is the Schlumberger configuration Fig.7a. To change

the depth range of the measurements the current electrodes are displaced outward after every measurement, while the potential electrodes are occasionally displaced when the ratio C_1C_2 : P_1P_2 is too large, otherwise, the potential difference becomes too small to be measured with satisfactory accuracy. Therefore, the distance between P_1 - P_2 must be less than$1/5^{th}$ of the current electrode separation. Two readings are necessary whenever P_1 - P_2 is changed for the same C_1-C_2 separation.

Another important electrode configuration, used less frequently in sounding, is the Wenner configuration (Fig.7b) and also the dipole electrode configuration has come in to use. All of these arrangements have the following in common; the distance between the two current and potential electrodes is very short whereas the distance from the pair of potential electrodes to the pair of current electrodes is considerably larger.

The basis for making VES, irrespective of the electrode array used, is that the farther away from a current source the measurement of the potential difference, or the curvature of the potential, or the electric field is made, the deeper the probing will be. It is designed to provide information on the variation of subsurface conditions with depth based on the variation of resistivity with depth.

Any of the electrode array used in electrical sounding may be used in horizontal profiling, but the data obtained with some types of arrays are more readily interpretable than data obtained with other arrays.

Further, the technique is particularly suited to detect the presence of horizontal or gently sloping beds of different resistivities. Even when the main interest may be in lateral exploration it is often necessary to carry out electric "drilling" at several locations in order to establish proper electrode spacing for the lateral search. Generally in VES with Wenner, Schlumberger or Dipole-Dipole, the respective electrode spacing A,L,S, is increased at constant logarithmic intervals and the value of the apparent resistivity $\rho_{a_W}, \rho_{a_{Sch}}, \rho_{a_D}$ is

plotted as a function of the electrode spacing on logarithmic coordinate paper. The curve of $\rho_a = f(A, L, S)$ is called an electrical sounding curve.

b) Horizontal profiling

In horizontal profiling one or two fixed electrode spacings are chosen and the whole electrode configuration is moved to a different location after each measurement is made. The value of the apparent resistivity is plotted at the center of the electrode configuration, and the results are presented as apparent resistivity profiles or maps. It is necessary, in profiling to use at least two different electrode spacing at each station in order to help distinguish the effects of shallow geologic structures from the effect of deeper ones.

The method is mainly used in mineral exploration in order to detect isolated bodies of varying resistivities, particularly, it is best suited to detect vertical dipping contacts and dykes of contrasting resistivity.

Another variation for this survey is the profiling by half-Shlumberger, where one current electrode is placed at infinity, and the two electrodes (single pole) array in which one current and one measuring electrode are placed at infinity.

3 . INTERPRETATION TECHNIQUES FOR RESISTIVITY SOUNDING DATA

The aim of geophysical interpretation of resistivity sounding is to determine the thickness and the resistivity of different horizons from studying, of VES field curves, and the use of these results to obtain a useful geological picture of the area under investigation.

Two methods by which resistivities and thicknesses are determined are discussed here. The methods are the DIRECT and INDIRECT approaches. The direct method provides procedures for obtaining the layer parameters directly from the apparent resistivity sounding measurements, (Slichter, 1933; Pekeris, 1940). More improvements have been made by using intermediate function (Koefoed,1968 and Ghosh, 1971a,b)

The indirect method involves the determination of the layer parameters simply by comparing the measured sounding with standard curves, or a model curve which is calculated from given layer parameters. It includes the curve matching methods, automatic forward and iterative methods. Curve matching methods includes complete curve matching, partial curve matching and asymptotic methods. Complete curve matching can be done with the help of available theoretical master curves. The automatic iterative methods are more efficient and are widely used nowadays, despite the fact that resistivity interpretations suffer from the same problem of non-uniqueness found with other potential field methods (Gravity and Magnetic).Details of the procedure followed are given in this section by first discussing the type of field curves.

3.1 STANDARED CURVES

From (2.21) one can see how the apparent resistivity varies for the different electrode spreads. When the electrode spacing is very small, that is, r » z, the series terms in all cases tend to zero, thus we measure the resistivity in the upper formation. On the other hand, since the reflection coefficient is less than unity, when the C-P electrode spacing is very large compared to Z, the depth of the bed, the series term will be

$$2\sum_{n=1}^{\infty} K^n$$

thus

$$\rho_a = \rho_1(1 + 2\sum_{n=1}^{\infty} K^n)$$

Therefore,

$$\rho_a = \rho_1(1 + \frac{2}{1-K}) = \rho_1(\frac{\rho_2}{\rho_1}) = \rho_2$$

That is to say, at very large spacing, the apparent resistivity is equal to the resistivity in the lower formation.

The master curves are prepared with dimensionless coordinates. Equation of apparent resistivity for all sounding configurations, obtainable from Equ.2.21 can be put in this form by dividing ρ_a by ρ_1 .The ratios ρ_a/ρ_1, are thus plotted against L/Z, L/Z that is, the electrode spacing divided by the depth of the upper bed for what ever electrode system is used. The curves are in logarithmic scales, that is, we are plotting (log ρ_a - log ρ_1) against (log a - log z).If we make ρ_1=1 ohm-m and z=1m,all the characteristic curves are preserved in shape, no matter what the multiplier is for the coordinates (ρ_a,L).The sets of

curves are constructed either for various values of K between or for various ratio of $\frac{\rho_a}{\rho_1}$

between $\pm \infty$

Two sets of theoretical two layer master curves are available for:

a) Set I : Ascending type ($\rho_2 / \rho_1 > 1$)

b) Set II: Descending type ($\rho_2 / \rho_1 < 1$)

Two layer standard curves prepared with a computer are available as an aid to interpretation. A typical set of two-layer curves published by Orellana and Mooney (1966) is shown in Fig.9.

Apart from the possibility that three layer, four-layer or in general multi-layer master curves could be drown with a computer using their corresponding formulae, the available two-layer curves could be used to plot three layer or four-layer curves for certain special cases.

The whole set of three-layer sounding curves are divided into four groups, depending on the relative values of ρ_1 ρ_a ρ_3

1. Minimum type or H-type ($\rho_1 > \rho_2 < \rho_3$)

2. Double ascending type or A-type ($\rho_1 < \rho_2 < \rho_3$)

3. Maximum type or K-type ($\rho_1 < \rho_2 > \rho_3$)

4. Double descending type or Q- type ($\rho_1 > \rho_2 > \rho_3$)

Different sets master curves for different values of ρ_2 / ρ_1 , ρ_3 / ρ_1 are given in Compagnie Generale de Geophysique, Anonymous and by Orellana and Mooney.

There can be only eight types of four-layer curves from a combination of the curves of the type H,A,K and Q. These are HA,HK,AA,AK,HH,KQ,QH and QQ. Theoretically plotted master curves for four-layer cases are available as 'PALEKA' in Anonymous by Orellana and Mooney also.

3.2 PARTIAL CURVE MATCHING AND THE AUXILIARY POINT METHOD.

Complete curve matching requires a large set of curves with a large number of parameters, needed to specify the contrasts in resistivities and ratio of thicknesses when more than two-layers are involved in the case of a single overburden, only one parameter is required, that is, the ratio of resistivity of the overburden and the bed rock. Therefore, it is difficult to compile a set of curves for more than two-layers which can satisfy the interpretation procedures. However, the interpretation is simplified by using partial curve matching with auxiliary curves. Particularly, the two-layer plus auxiliary curve method which is based on the assumption that any three layer resistivity section can be analytically expressed as an equivalent two layer section. This approach is widely used to approximate a layer model which can be used as starting model for an automatic iterative or forward interpretation. The detailed description of the methods are given in (Koefoed, 1978)

In partial curve matching, short segments of the apparent resistivity curve starting from the shorter spacing and working towards the layer spacing are interpreted using two layer master curves. As each portion of the curve is interpreted, the layers of the interpreted section are combined together to form a fictitious uniform layer with a combined resistivity ρ_e and a combined thickness, h_e. This fictitious layer then replaces the surface layers when the next portion of the curve is interpreted. As each portion of the curve is interpreted, the origin of the two layer master curve represent the fictitious layer that replaced the top two layers. To define the resistivity and thickness of each layer, a relation between the parameters of the fictitious layer and the top two replaced layer has been developed for various types of model curves. The relationship between fictitious and real layer parameters differs with the type of curves. There are four possible types of sounding curves for three-

layer models. These mathematical expression for each types of model curves can be found in Keller and Frischknecht (1966).

Step-wise reduction of multi-layer curves to equivalent two or three -layer cases renders possible their interpretation with the help of available two- and three master curves and complementary curves known as auxiliary point charts. The coordinates of the Auxiliary curves are the ratio of the real layer and the ratio of the resistivity of the fictitious layer and the first real layer.

All the auxiliary curves are on a logarithmic scale with the same modulus used for the apparent resistivity curve (Fig. 10 and 11). With this method, only approximate models can be obtained and the accuracy decreases with the number of layers in the sounding curve.

In the final analysis, however, the best approach is to directly calculate theoretical sounding curves and compare them with the observed sounding curves.

SHEET
LAMINA 1

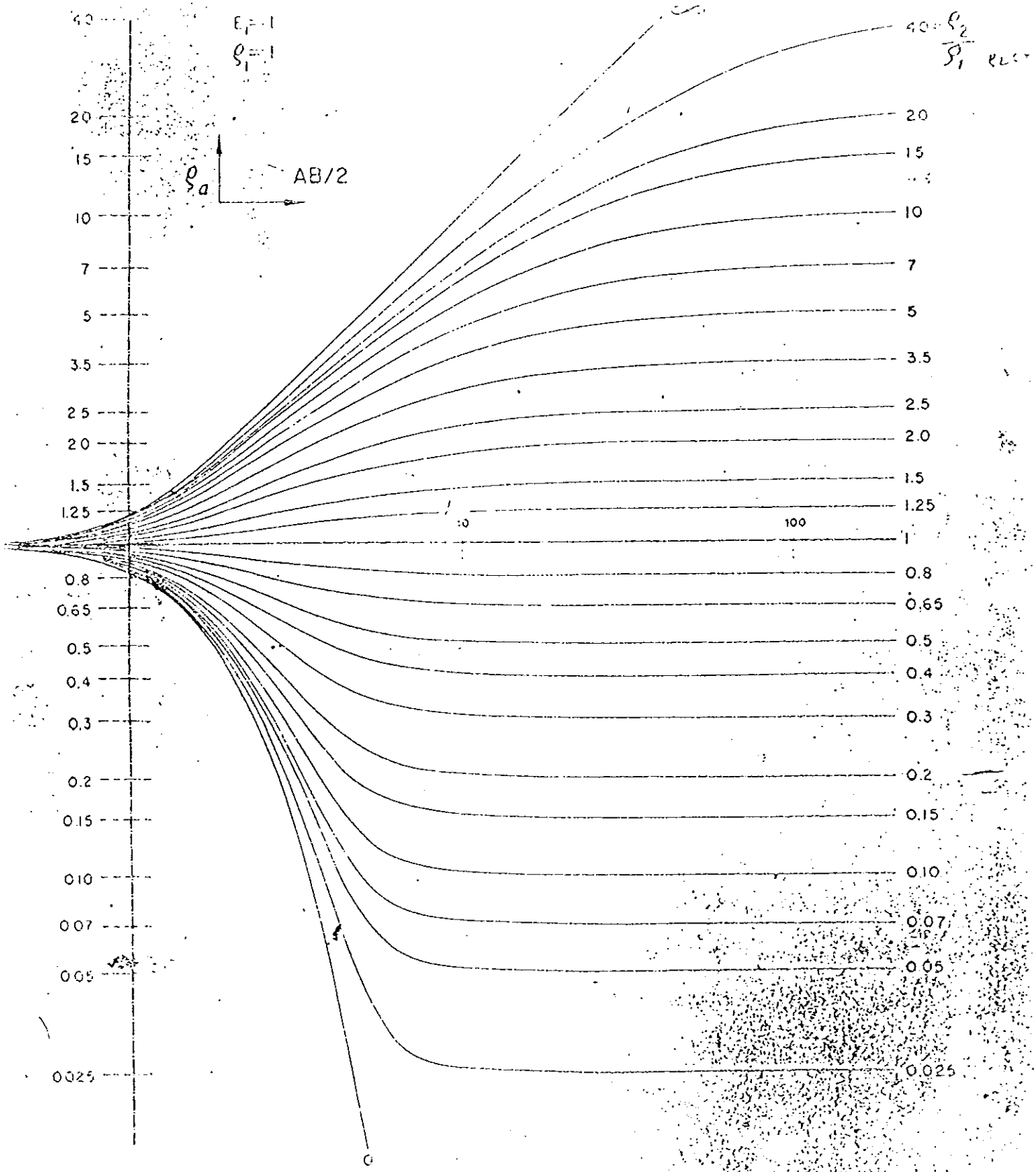

TWO — LAYER CURVES — CURVAS DE DOS CAPAS

AUXILIARY GRAPH (A-TYPE)
GRAFICO AUXILIAR (TIPO-A)

SHEET-B
LAMINA-B

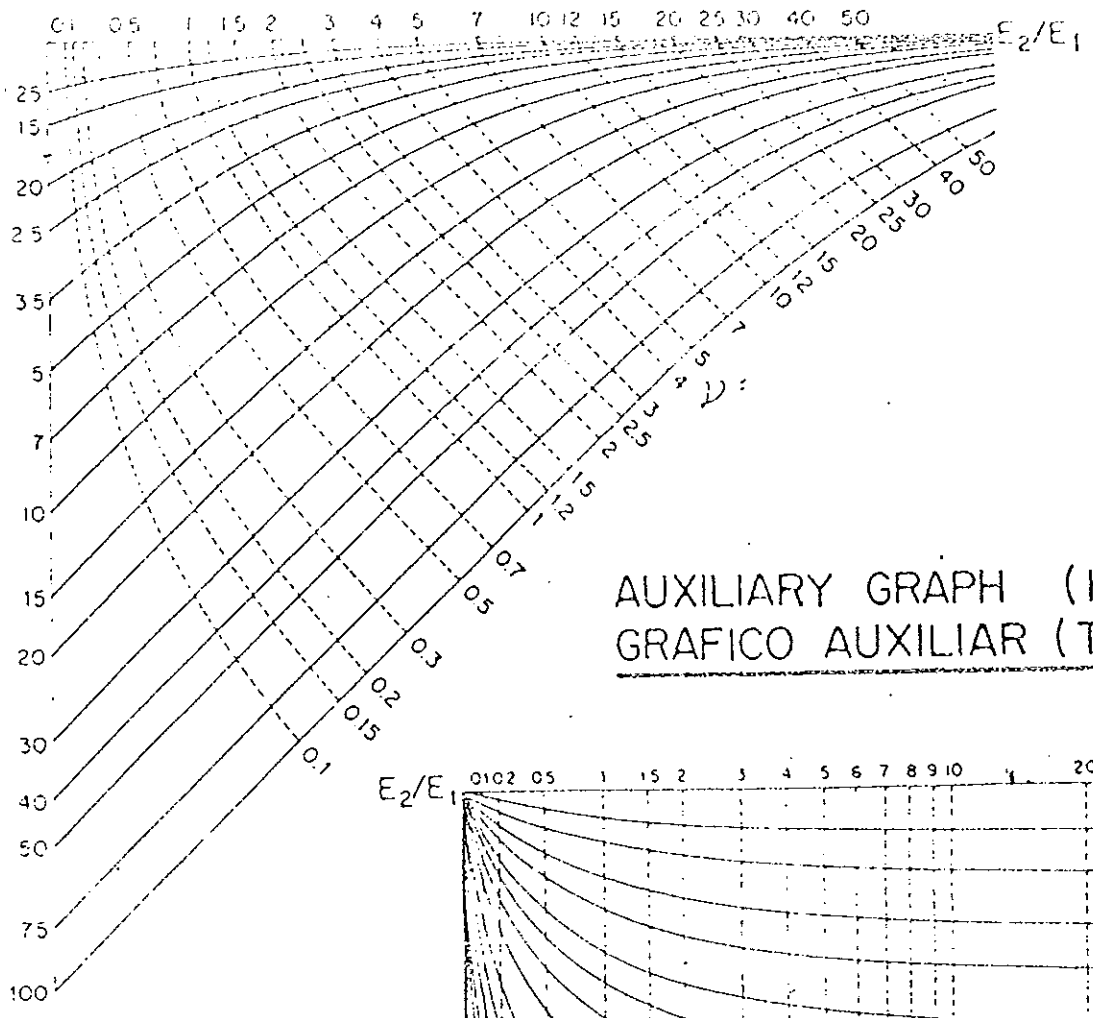

AUXILIARY GRAPH (H-TYPE)
GRAFICO AUXILIAR (TIPO-H)

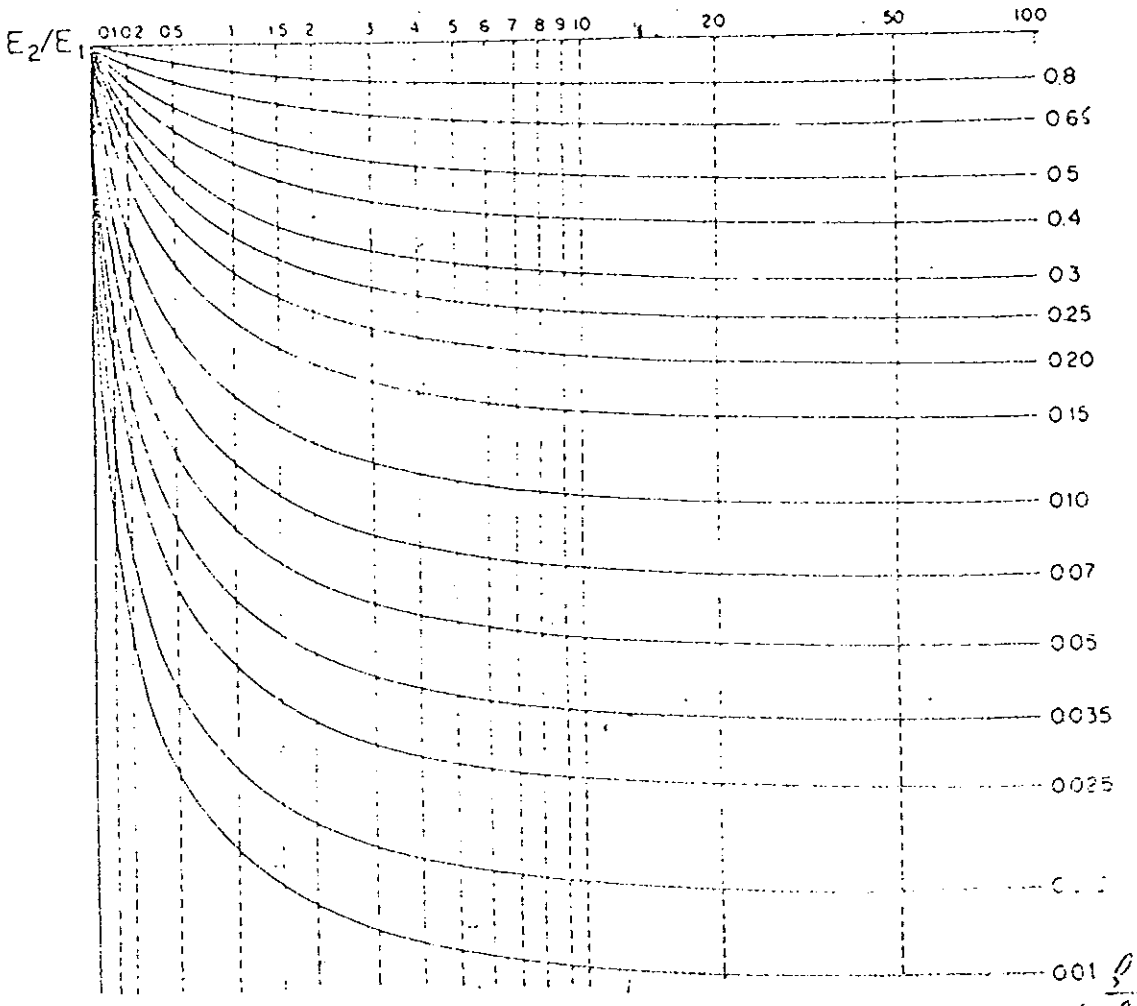

AUXILIARY GRAPH (K-TYPE)
GRAFICO AUXILIAR (TIPO- K)

SHEET - A

LAMINA - A

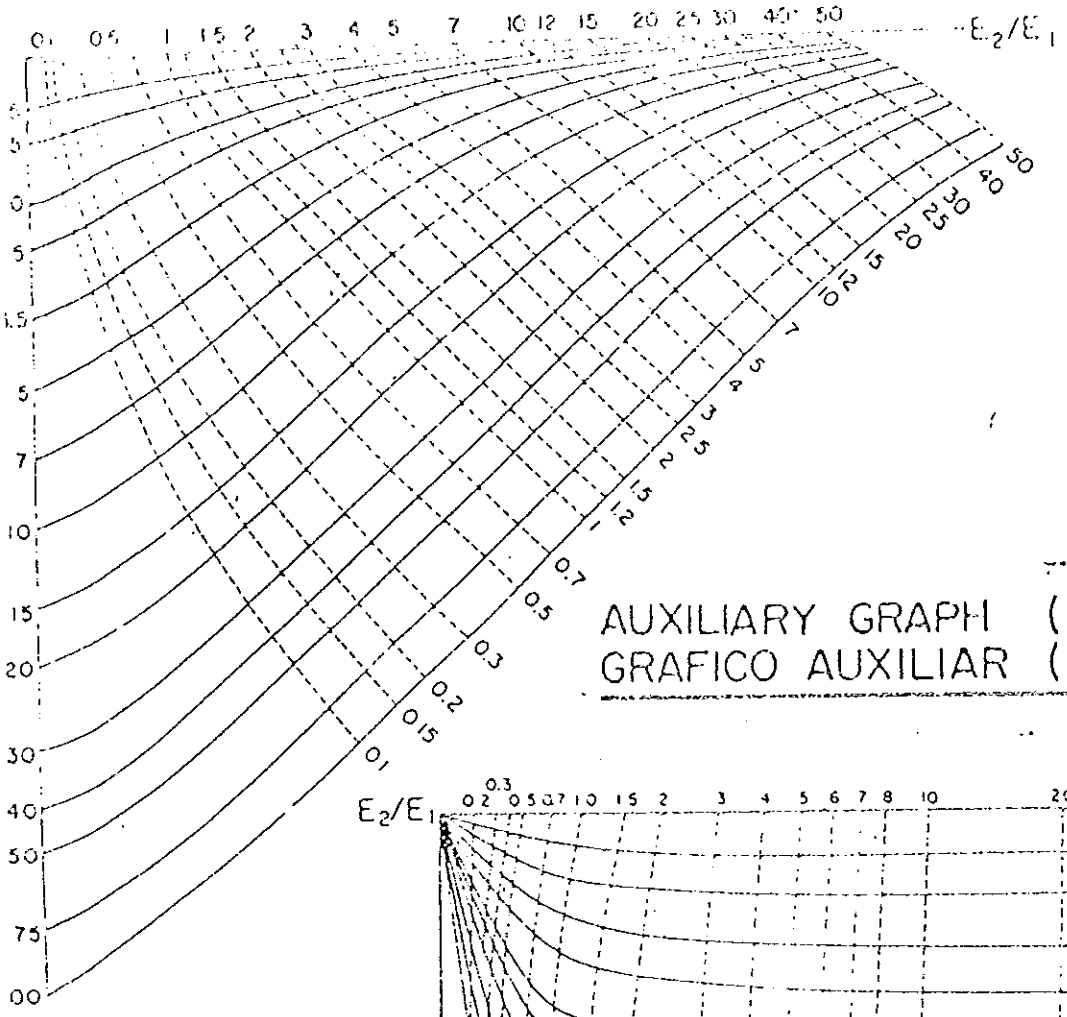

AUXILIARY GRAPH (Q-TYPE)
GRAFICO AUXILIAR (TIPO- Q)

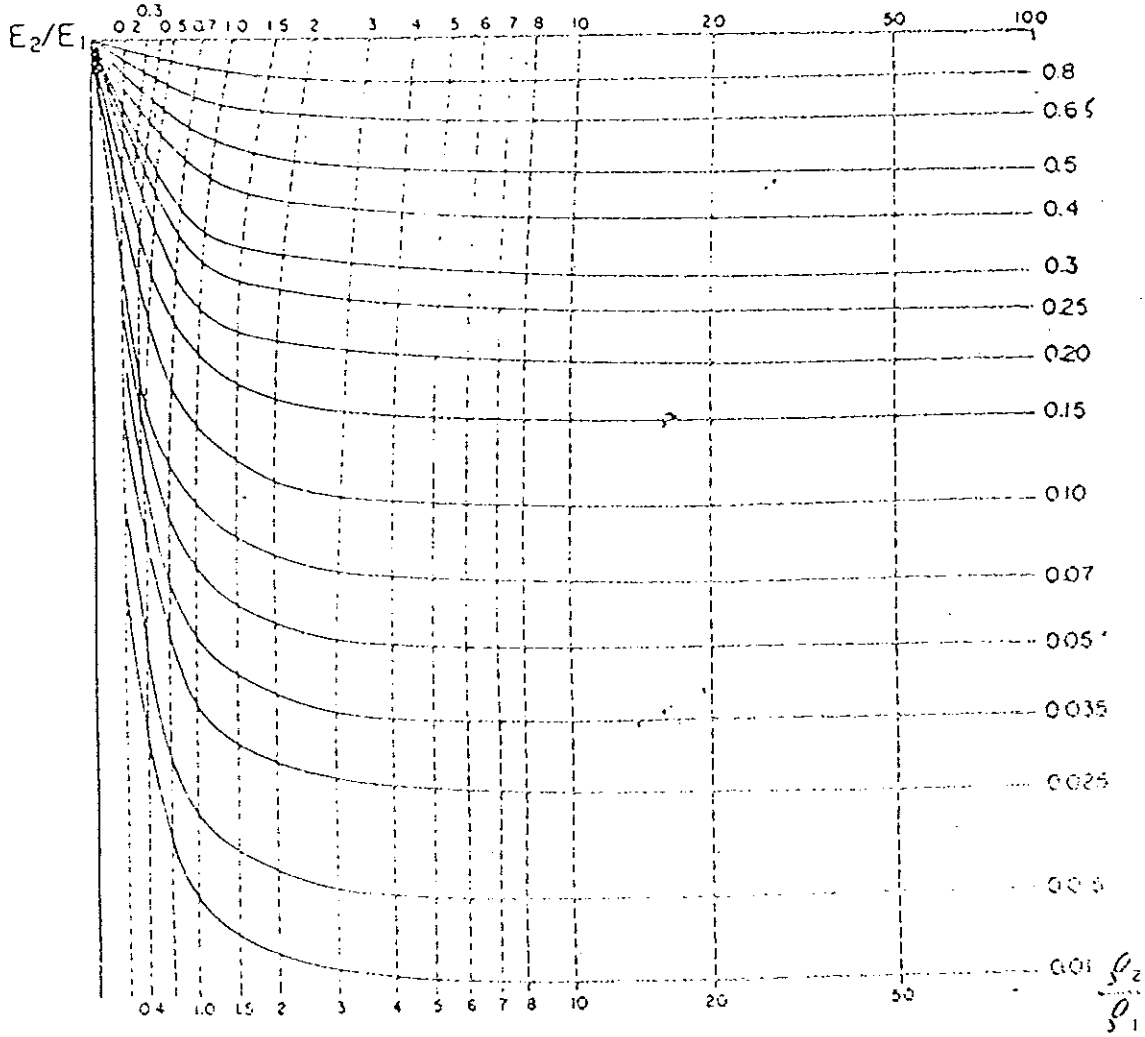

ORELLANA - MOONEY

3.3.1 Forward Modeling:

The method has been used for many years, and nowadays usefulness is outweighed by inversion methods since it is time consuming and tedious, particularly when several layers are treated. For the starting model, the auxiliary point method with additional geological information may be used, but adjustment of layer parameters is made manually and changes in the parameters are based on subjective judgment. Concerning the amount of the change in the value of the layer parameter, Marsden (1973) showed the possibility that any resistivity sounding fit can be made by a fictitious stack of layers with geometrically progressing depth to the interface. He stated that a linear relationship exists between the relative changes of a layer parameter and the resulting relative changes in the value of the apparent resistivity. The amount of difference observed between the field and the model apparent resistivities leads to an estimation of the amount of modification to be made on the layer parameters.

The method is time consuming, however, with a good initial starting model fairly fast and accurate solutions can be obtained.

3.3.2 The Inverse Approach/Automatic Iterative Interpretation Techniques

Since 1973 various authors have published methods of automatic interpretation; in which the computations of the layer parameters are made by computer. At present the iterative methods are the most widely applied tool in the interpretation of resistivity sounding measurements. The decision regarding the adjustments of layer parameters are made by a computer to get the best fit between measured and calculated curves.

In this work the final interpretation of all sounding measurements has been made using a non-linear least square inversion computer program (SEV) which can utilize two algorithms for calculating the resistivity of a given one dimensional model. The program requires equally distributed data with respect to AB/2 on a logarithmic scale with 10 points per decade. It involves computation of data and model parameters using a logarithmic scale so that the severity of nonlinear dependence of the apparent resistivity on the model parameters is reduced as compared to a linear representation.

In the adjustment procedure, the number of layers during the iteration process will not be changed but the program has the option of assuming a fixed value for the layer parameters (thickness and resistivity) which is extremely useful when one or both of these parameters is already known.

The quality of fit between measured and calculated apparent resistivity values is measured by the standard deviation, that is, the lower RMS error the better the fit. The fit also depends on the initial guess of the layer model.

3.4 Depth of investigation in direct current surveys

Depth investigation is a basic physical concept in any geophysical prospecting. It has a precise and clear meaning for fields which involve propagating signals in which different depths give rise to separate signals on the record. But, for fields with no signal propagation such as electrical fields, the meaning becomes vague and it is difficult to pinpoint the depth of investigation. In the artificial methods of D-C electrical prospecting the voltage measured between the potential electrodes is the sum of the contribution of the earth material from different depths. It is obvious that the ground layers from different depth do not contribute equally to the total measured signals. Roy and Apparao (1971) defined the depth of

investigation in any direct current resitstivity method as that depth at which a thin horizontal layer contributes the maximum amount to the total measured signal at the ground surface.

For a long time the depth of investigation has been considered synonymous with the depth of current penetration or their distribution. But, the current penetration or distribution is a function of only the position of the current electrodes where as the depth of investigation is determined by the position of the potential and current electrodes.

A number of workers defined the depth of investigation differently. Roy and Apparao have suggested the following values for the absolute depth of investigation in homogeneous ground in terms of L, the distance in any configuration between the two extreme active electrodes.

Electrode configuration	Depth of investigation
Wenner	z= 0.11 L
Schlumberger	z= 0.125 L

values for other electrode configuration are also given, but these are taken as an example. It shows a different depth of investigation for the same spacing between the current electrodes and the same current penetration and distribution. It's significance is that it can provide a general guide to choose an electrode system and it's spacing for any real inhomogeneous problem.

Edward (1977) concluded that the definition for depth of investigation given by Roy and Apparao (1971) to describe the effective depth of investigation was not the best choice. Rather, he preferred "the median depth", Z_{med}. That is, the effective depth which is defined to be the depth at which exactly one half the total signal originate from above and one half from below. Effective depth values for various arrays are expressed in terms of the current electrode separation (L) and the measuring electrode distance (a). The Wenner and the Schlumberger values are given below:

Electrode Configuration	Depth Of Investigation
Wenner	0.173 L
Schlumberger:	
ideal $a \rightarrow 0$	0.192 L
L=4a	0.192 L
L=20a	0.191 L
L=10a	0.190 L

For the Schlumberger array, the depth is directly proportional to L and nearly independent of a. This means (a) can be chosen to be any convenient value which gives a sufficient signal for an expanding electrode length (L).

The normalized contribution of a layer of homogeneous isotropic ground is a function of the array length and depth Z of the layer and it is different for different electrode arrays.

Although there is no limit to the depth to which studies may be made since by increasing the electrode arrangement a desired depth may be studied, in practice technical difficulties exist which affect the correct measurement of potential drop. The main effects other than the resistivity inhomogeneity are skin effects, alternating current and induction phenomena.

3.5 PRINCIPLE OF EQUIVALENCE AND SUPPRESSION

Equivalence and suppression are two basic phenomena which cause ambiguity and a non-unique solution in resistivity interpretation. Equivalence refers to the condition in which different combinations of layer resistivities and thicknesses may lead to apparent resistivity

curves which are within the accuracy of observation are indistinguishable although not identical.

Suppression refers to the condition in which the effect of an intermediate layer (thickness very small compared to its depth) in an apparent resistivity curve of ascending and descending type is small that its detection from the curve may be impossible.

When different sets of layering parameters provide the same sounding to within 5%, these sets of conditions are said to be equivalent (Keller and Frischknecht, 1966). The limit of 5% is the accuracy with which measurements can be made and it can arise from variations in near surface resistivity. Koefoed (1979) considered the error limit of 2% in the resistivity transform within which equivalence can exist. Maillet (1947) obtained two simple groups of equivalence: the first one refers to a bowl-type (H) or ascending-type (A) resistivity sequence in which the resistivity of the middle layer is very small compared to the layer immediately below it. In this case equivalence for the middle layer is maintained provided that the longitudinal conductance remains constant, that is, the ratio of its thickness to its resistivity h_i/ρ_i. The second group of equivalence refers to a bell-type or descending type (Q) resistivity sequence in which the resistivity of the middle layer is much larger than the layer immediately below. In this case equivalence is maintained provided that the transverse resistance of its thickness and resistivity $(h_i \rho_i)$.

The range of variation of layer parameters maintaining equivalence has been studied by a number of workers as it can provide lower and upper values to certain layer parameters if no other subsurface information are available.

4 . DATA ACQUISITION, PROCESSING AND PRESENTATION

The collected field data's composed of instrument readings [voltage (V_P)] from the receiver and current (I) from the transmitter. The first step of data processing is the transformation of the field data to the apparent resistivity (ρ_a) value using the relation given in Eqn.2.20. This apparent resistivity data is not in a form that it can be readily interpreted, therefore, reductions are applied so that to some degree acceptable interpretations can be made.

4.1. FIELD INVESTIGATION AND INSTRUMENTS USED

The topography in the area of survey is completely flat and it is 1140m above sea level.

In order to get an idea of the geological sequences and the associated resistivity values 16 vertical Electrical Sounding (VES) measurements were taken applying Schlumberger electrode configuration, along three profile lines reach 1km long at an average line spacing of 200 m and each of the profile lines were oriented in E-W direction as indicated in Fig.12. At every VES station the orientation of electrodes spread was made more or less in the same direction so as to minimize resistivity variations that may due to anisotropic nature of the subsurface formation.

The resistivity sounding was done at intervals of 150m with the following electrode spread positions. For the current electrodes, the spread positions (AB/2) in meters are: 1.5, 2.1, 3.o, 4.2, 6.0, 9.0, 13.5, 20, 30, 45, 66, 100, 150, 220 and 330. The potential spread

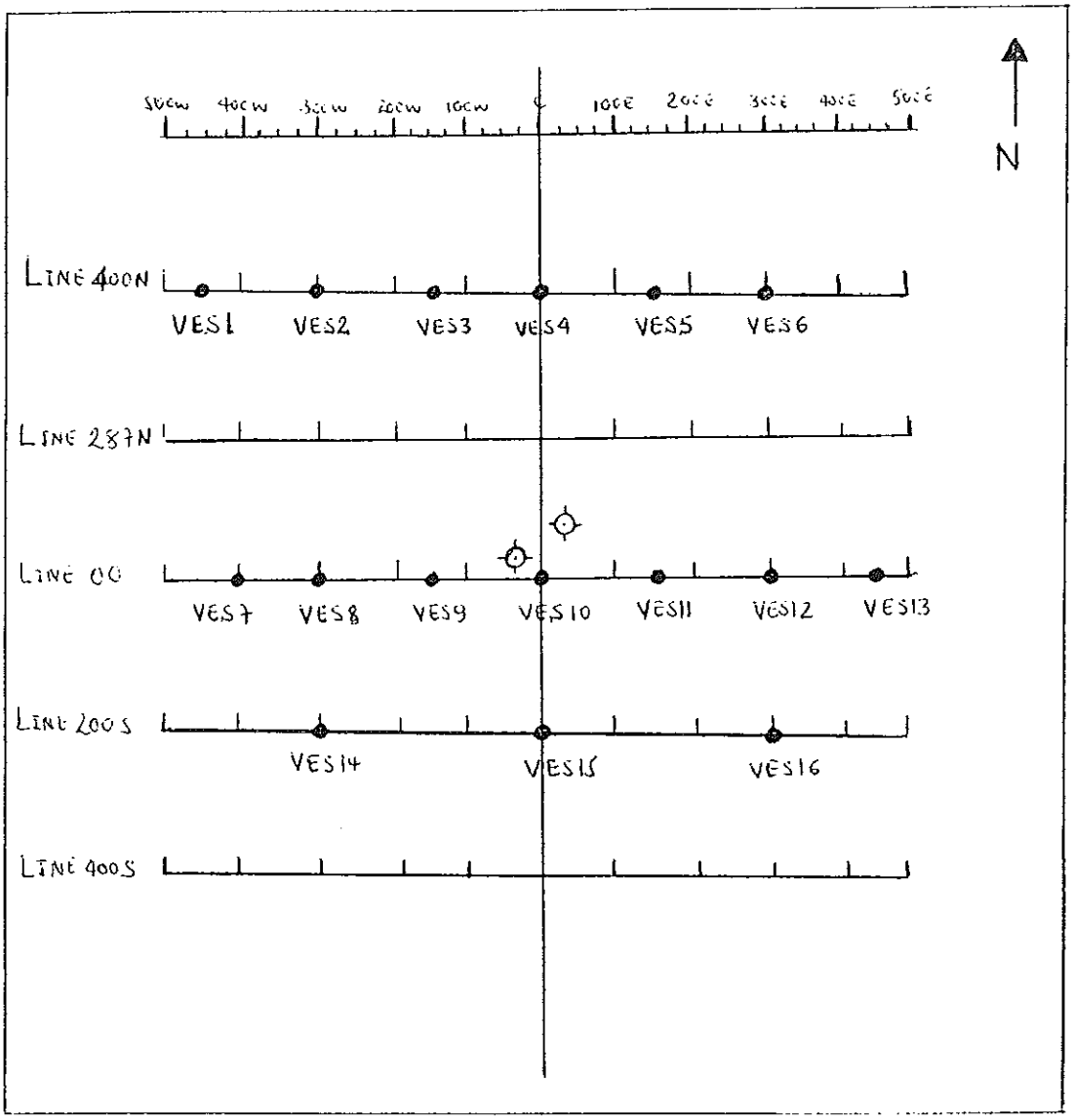

Fig. 12: Location of Survey lines And existing boreholes

LEGEND

⊙ Existing Boreholes

BH-1 Moyale Well # 88-1

BH-2 Moyale Well # 88-2

• VES Location

Scale 1:10,000

positions (MN) in meters are: 1.0, 12.0 and 90. Overlap measurements were made at AB/2 = 20, 30, 150 and 220.

All sounding data measurements were made using IPR-8 Receiver, TSQ-3 Square Wave Transmitter which generates a regulated DC voltage, 8HP Briggs & Stratton motor generator which supplies power to the Transmitter, copper and stainless steel electrodes for transmitting current into the ground and for the measurement of the potential difference and a number of reels with a capacity of 500m of cable for current and 250 m for potential spreads. Sufficient care was taken to ensure good contact with the ground. Porous pots with saturated copper sulphate solution were also used for potential electrodes in order to get a good electrical contact at some location. The signals were set for the same period (2s) as the transmitter. The receivers were calibrated at every station to offset self potential noises. During the survey proper care was taken to prevent interference from self-potential, polarizing effects, contact errors and other disturbances for the potential gradient measurements in each sounding.

The row data which were collected in the field are given in Appendix A.

4.2 DATA REDUCTION

For data processing of the Sounding the apparent resistivity values are plotted on logarithmic transparent paper, the apparent resistivity values on the ordinates and the electrode separation (AB/2) on the abscissa. But, the resistivity measurements are made by progressively increasing the potential electrode distance (MN) for relatively large increment of the current electrode distance (AB/2). Thus, in most cases the sounding curve is segmented and can not be interpreted as it is . Precise interpretations requires knowledge of the causes

which affected the shift, so that the effect can be quantified and corrections can be made in order to obtain a single smooth curve.

The ideal condition with the Schlumberger method is that potential electrode spacing be infinitely small compared to the current electrode spacing. Therefore, when potential electrode positions are shifted and the requirement is not maintained, the form of the actual apparent resistivity curve may be changed. Thus, two effects can be attributed to the effect of the displacement of the segment: 1) the change in the geometry of the configuration because that ratio MN/AB can no longer be assumed to be infinitely small and 2) in homogeneity of resistivities near the potential electrodes.

Accordingly, in this work, correction for these effects has been made for all sounding stations by using a computer software program "SEV" which utilizes a statistical data correction procedure (Prof. Roberto Ballia).

4.3 DATA PROCESSING AND PRESENTATION

After data reduction of each sounding curves, the data are processed. To determine the layer parameters, thickness and resistivities in the survey area, curve matching (Two-layer plus auxiliary curve) techniques (Orellana and Mooney, 1966) and the automatic iterative method were applied.

The initial model parameters which were obtained by the auxiliary point method were used to obtain good starting models for one dimensional inversion of Schlumberger resistivity sounding by the computer soft ware program "SEV", and then the first model parameters were improved through an iterative process of curve generation and fitting procedure of the program. All sounding data have been interpreted using this program. The fitting of all observed and calculated values were based on the data and the available subsurface geological

and bore hole information. During data processing, the ranges of equivalence were evaluated. As already discussed in the principle of equivalence and suppression in section (3.4 and 3.5), different model solutions can be obtained for an equivalent interpretation. Considering a 5% ordinary error limit in the measured data, the limit of equivalent solutions for the model parameters were assessed for some sounding curves and presented in appendix B. The results of the model interpretations of each sounding's curves are presented in the same appendices.

The depth/thickness and resistivity parameters acquired by iterative interpretation of sounding curves were used to construct geoelectric sections for each profiles to show the distribution of different lithologic units both in horizontal and vertical directions. Apparent resistivity pseudosections were prepared by plotting the measured apparent resistivity values of each progressive electrode position below the center of the electrode spreads for each profiles to assess the vertical resistivity variations. Moreover, to observe the subsurface lateral resistivity variations, apparent resistivity maps for constant electrode spread positions of AB/2 = 45 m and 100 m were plotted by using the measured resistivities at each stations and these selected electrode positions. These values were contoured by using computer Software program. This program was applied for the mapping of the geoelectric sections and the pseudosections for each profiles.

5. INTERPRETATIONS OF GEOELECTRICAL RESULTS

The resistivity-depth distributions yielded by the data analysis program for each sounding was used together with borehole data and general knowledge of the regional geology and geophysics to develop the final interpretations of the distributions of subsurface layer by which the geoelectrical sections were determined.

5.1 GEOELECTRIC SECTION ALONG PROFILE ONE

This profile line includes six VES stations (VES1 - VES6) and extends to a total length of about 1 km. The separation between any two consecutive VES points are 150 m.

The geoelectric sections of this profile line were constructed from the interpreted data of the individual sounding stations (VES1 - VES6) to better illustrate the vertical and lateral distribution of resistivity across this profile line (Fig. 13).

The result of sounding survey has revealed that the apparent resistivity curves along the profile line are found to represent a model having five geoelectric layers. The geoelectric layers consisting the top most part of the session are characterized by minimum thickness and high apparent resistivity ranging from 100 to 470 ohm-m in the vicinity of VES2 and VES3 and it decreases to about 46.5 ohm-m around VES4 and VES5. The thickness of the layer is within the range of 0.35 - 0.76 m and it is relatively thick around VES4- VES6. Taking into account visual field observations and borehole information, those high resistivity values are attributed to clay or slity-clay that cover the upper part of the lithologic succession.

The second layer shows resistivity values ranging from 30 to 49 ohm-m and this layer attain its maximum thickness, which is about 10 m, in the vicinity of VES3 and VES6, and its minimum 1m, around VES1. Geologically, it is classified as Marl and Marly limestone containing high moisture contents.

The third layer shows lateral resistivity variation and it represented by a higher resistivity response 100-169 ohm-m in the region between VES1 and VES4 and a relatively lower resistivity response (50 ohm-m) in the region between VES4 and VES6. This layer attains its maximum thickness, which is about 20 m, in the vicinity of VES3 and VES5, and its minimum 5 m, around VES4. This high resistivity region can be represented by fractured and wet sandy limestone. Whereas the low resistivity region may be described as the response of the weathered bedrock, because the bed rock is obtained at shallow depth around these VES.

The fourth layer as delineated by resistivity responses appear to represent two different lithologies separated by a certain type of tectonic feature, probably a fault plain. On the Western part of the traverse a relatively low resistivity section in the ranges of 17- 52 ohm-m, terminated around VES4, and then comes a high resistivity formation (340- 490) ohm-m which seems the uplifted part of the underlying bed rock. Moreover, the resistivity response of the overlain layer around this part displays almost the same value and this might be ascertain the existence of a fault plane around VES4 (Fig.13). The low resistivity values 17-50 ohm-m detected in the western part of the traverse are indicating the conductive nature of the subsurface formation. From the hydrogeological point of view, this part of the layer appears to deserve more interest for groundwater exploration.

As to the borehole geological log data, in the survey area the water-bearing horizons (aquifers) are found to be represented by sandy gravel or gravely sand beds. Thus, this low

resistivity range detected on the Western part of the traverse interpreted to be a response of saturated sandy gravel or gravely sand, and hence deserves much interest for ground water exploration. But, the high resistivity contrast observed on the Eastern side of the traverse could be due to the uplifted Biotite schist comes to be right beanth the second weathered schist layer or sandy limestone.

The fifth layer is represented by a higher range of resistivity response and outlines the bottom basement rock which is the fresh bedrock. From station to station the depth to this bed rock shows a considerable variation of resistivity. For example, in the vicinity of VES1 the depth to bed rock was estimated to be in the range of 45 to 50 m, around VES2 in the range of 60 to 65 m which is relatively deeper than the other stations, and the depth in vicinity of VES3 is in the range of 40-45 m which is shallower as compared to the other stations And thus the thickness of the overlying sediment is thicker in the vicinity of VES-1 and VES-2 and becomes thinner in the Western and Eastern part of the transverse line Therefore, from this we can infer the morphology of the bed rock is undulated.

The resistivity values of the Biotite Schist bed rock vary from 520-1800 ohm-m in the Western part of the transverse and vary from 340-490 ohm-m in the Eastern side of the line. These contrasts may be explained to arise due to variations in composition, degree of weathering and texture.

The apparent resistivity distribution on pseudo-section map of profile 1 (Fig. 14) exhibits a gradual increasing trend from West to East and then a decreasing trend to East. From the Western flank up to 300 E, the closed low resistivity zone in the middle portion of the sections seems the response from the Sandy gravel and Gravely sand. Further to East the resistivity increase and qualitatively demarcates the boundary, where the horizontal extent the section stops.

Regarding the structure of the bed rock, at 150 E and 450 E the depth to the bed rock is deeper than the other part. This is an indication of undulating structure of the basement on the pseudo-section, and also the relatively uplifted portion of the basement in the vicinity of 600 E and 750 E is shown. But a clear demarcation of the uplifted part is not displayed on the pseudo-section.

In general, the geoelectrical section from VES parameters of profile 1 depicted lithologic variations. Accordingly, the layers categorized in the fourth group with resistivity range from (17-52) ohm-m are expected to be the likely host of groundwater. These resistivity ranges are indications of sand and Sandy-gravel beds which are considered to be the favorable lithological unit for accumulations of fluids in their pore spaces. And also analyzing the geoelectric section, the aquifer is thicker and deeper around VES 1 & VES 2 and it becomes thinner towards the Eastern side of the line. Thus, the undulating structures of the basement and the presence of shallow and deep of the aquifers probably indicates the undulating nature of the buried river channel along the corse.

As observed on the sections, almost all layers are showing a drastic resistivity change when crossing the vicinity of VES 4. This may be due to the presence of fault or fracture resulted in the uplifted of the basement or it may be due to the variation in the degree of the weathered basement.

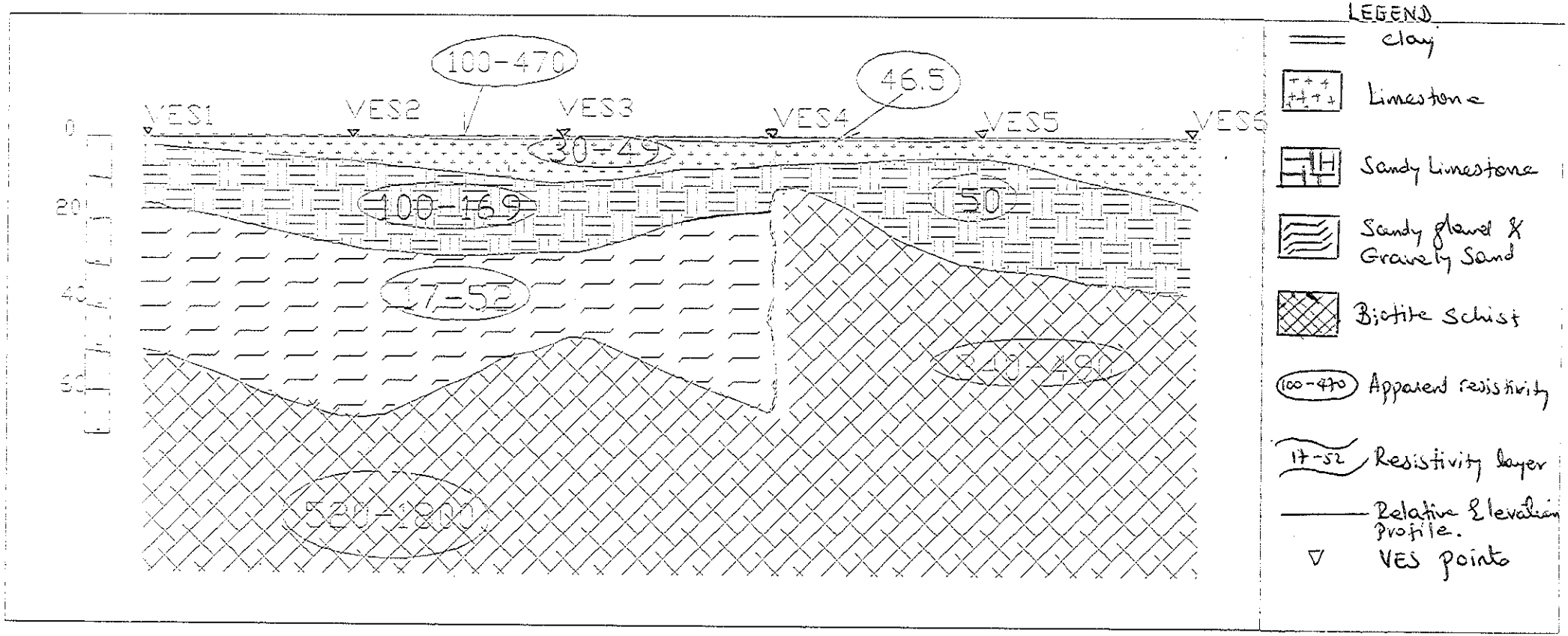

Fig.13 Geoelectric Section Along Profile 1 El-Gof

Fig.14 Apparent resistivity Pseudo-Section of Profile 1

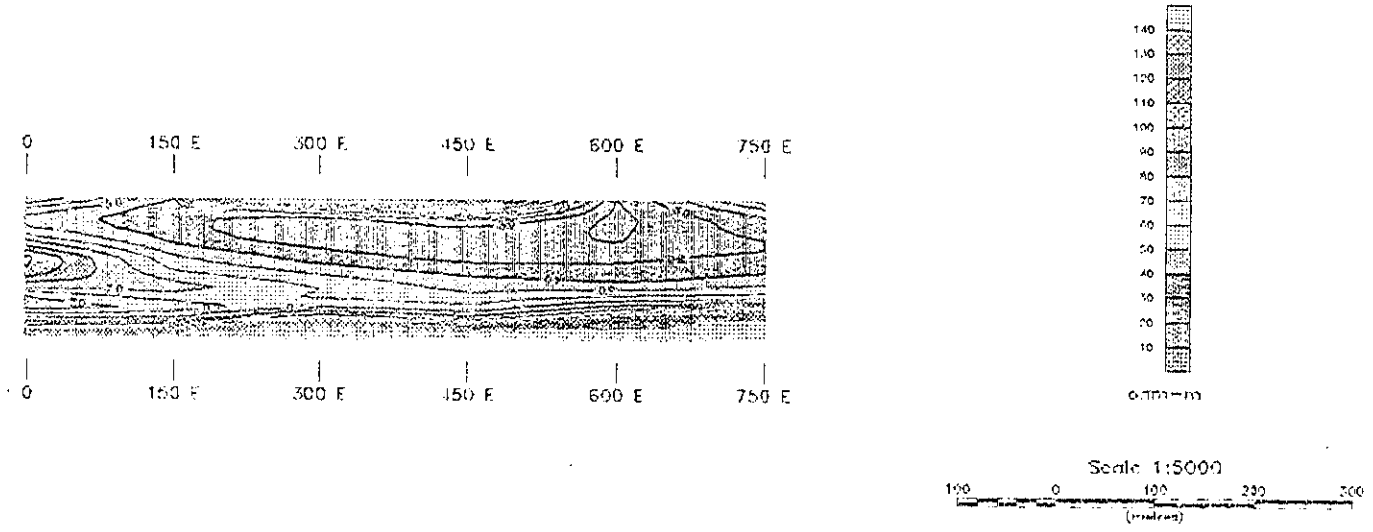

5.2 GEOELECTRIC SECTION ALONG PROFILE TWO

This profile line found at a distance of 400 m South of profile 1 and stretches to a total length of about 1 km and placed parallel to the first profile line (Fig. 15).

Seven Soundings, VES7-VES 13, were taken along this profile. The stations interval are the same as that of the profile one, except between VES 7 and VES 8 which is 100 m.

The geoelectric section prepared on the basis of results of each sounding, five geoelectric layers could be differentiated. The top most layer is found to be thin (maximum 0.8 m) and shows a considerable resistivity variations from station to station. The resistivity response in the vicinity of VES 7- VES 9 is varying in the range 190-276 ohm-m and around VES 10 and VES 12 varying in the range 670-1000 ohm-m and in between VES 11 and 12 it is found to be 488 ohm-m, whereas in the vicinity of VES 13 decrease to about 29 ohm-m. Geologically it is classified as Slity clay and loose sand.

These resistivity contrast may be explained to arise due to variations in composition, moisture and clay content.

The second layer shows a resistivity response varying from 20-26 ohm-m. Geologically, it may correspond to Marl and Limestone horizon having relatively high moisture content. The maximum thickness is determined at VES 16, which is about 15 m and thins out towards VES 13.

The third layer shows a considerable resistivity variations from station to station and its thickness ranges from 25-45 m. This layer is characterized by a higher resistivity 60-90 ohm-m to the Western part, and 105-125 ohm-m to the Eastern part of the transverse and moderate resistivity 40-60 ohm-m in the regions between VES 9 and VES 11 and by a low

resistivity 25 ohm-m in the vicinity of VES 8. The patterns of the horizontal resistivity variation is from high to low and from low to moderate and to high.

The low resistivity in the vicinity of VES8 is interpreted to be a response of saturated Sandy gravel and Gravely sand bed, in contrast, the highest resistivity range 105-125 ohm-m detected at both ends of the line is attributed to the response of the weathered Biotite Schist bed rock. The overall thickness of this layer varies from 25 to 35 m. Therefore, the low resistivity portion of the horizon considered to be the favorable aquifer zone, and hence deserves much interest for groundwater exploration.

The bottom layer showing a resistivity range of 280-880 ohm-m in the region between VES 7 and VES 11, and a resistivity of 450-1000 ohm-m between VES 11 and VES 13.

The variation of resistivity value of the bed rock may be due to variations in composition, degree of weathering, etc. Along this profile the depth to the bed rock is predicted to be 80 m below land subsurface in the vicinity of VES 8 and VES 9, the bed rock shallows to approximately 50-60 m below land subsurface around VES 12 and VES 13. This depth to the bed rock variation from station to station indicates the undulating nature of the bed rock morphology.

On the pseudo-section map of profile 2, Fig. 16, the resistivity contour lines distribution exhibits a gradual increasing trend towards the top layer. The resistivity of this middle layer increases towards the East but starting from 150E to the West the resistivity becomes very low, however, in the region between 150E and 100E relatively low closed resistivity contour value displayed. The thickness of this layer is thicker to the Western end and thin out towards the East. The low apparent resistivity outlined by contour values less than 50 ohm-m in the western part reflect the response of the sand and gravel deposit.

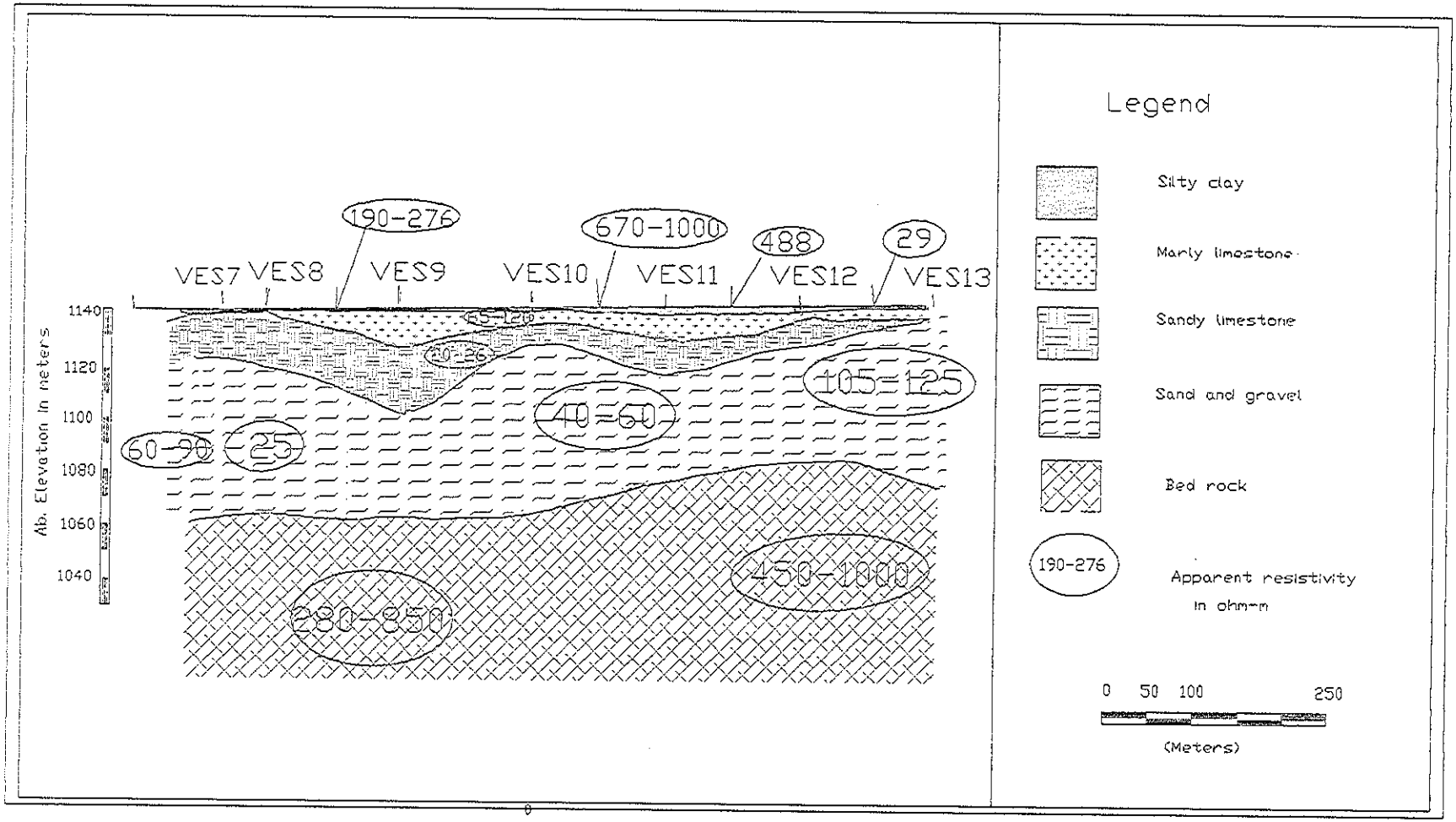

Fig.15 Geoelectric Section Along Profile 2, El-Gof

Fig. 16 Apparent resistivity pseudo-section of profile 2, ES-E of

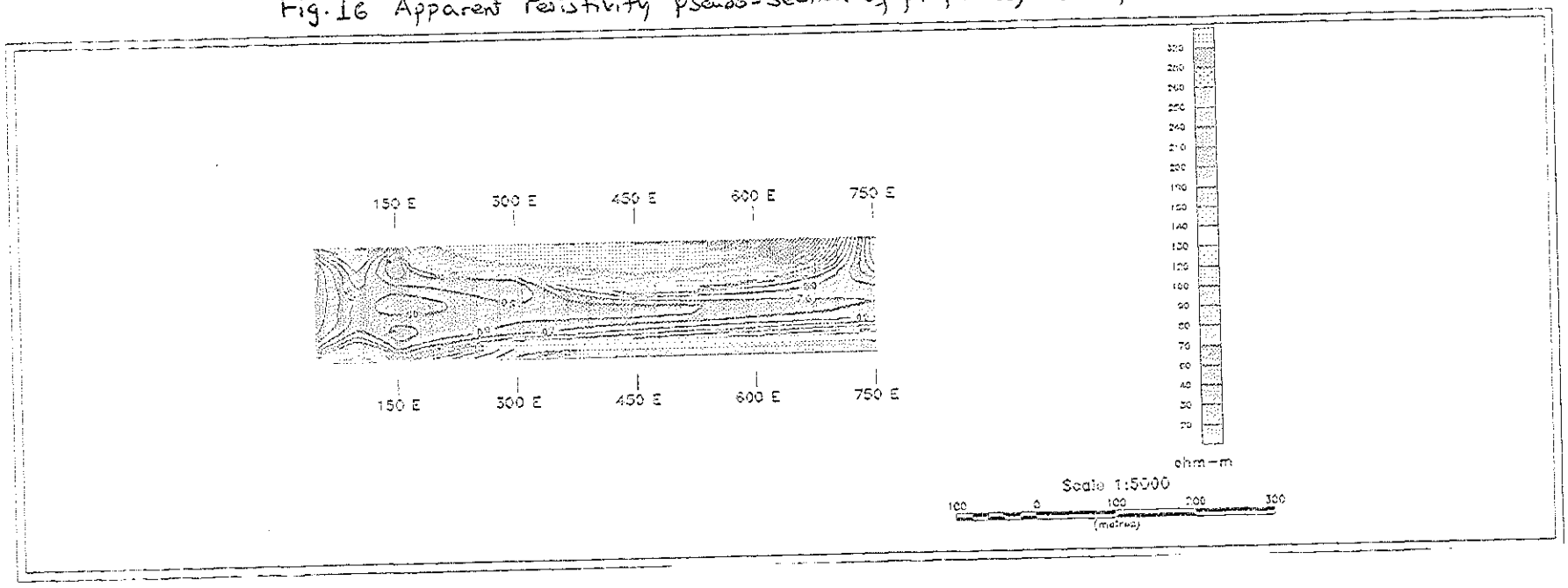

5.3. GEOELECTRIC RESULT ALONG PROFILE THREE

This profile line includes three VES stations VES 14 -VES 16, and extends to a total length of about one km. The separation between each VES points is about 150 m.

The vertical section shown in Fig. 17 displays five geoelectrical layers. The top layer is characterized by a resistivity range of 165-800 ohm-m. The highest range 360-800 ohm-m was detected between VES 14 and VES 15, and the lowest 165 ohm-m in the vicinity of VES 16. The variation of the top layer resistivity is most likely due to the variations in its grain size, moisture and clay content, and composition. Geologically, it is classified as Slity clay soil. The overall thickness of this layer varies from 0.4 to 0.7 m through out the transverse.

Beneath the above discussed layers is a relatively low resistivity horizon with values ranging from 13-42 ohm-m. Unlike the above layers, this one shows a uniform resistivity distribution. The thickness of this layer found to vary from 9 m, at VES 14, to 8 m around the region between VES 15 and VES 16. This low resistivity horizon is attributed to saturated Marl and Marly limestone. The third layer showing a uniform distribution of resistivity ranging from 72-92 ohm-m. The maximum thickness attains about 15 m, at the vicinity of VES 15, its minimum 6 m around VES 16.

The forth layer shows a uniform resistivity response varying from 40-70 Ω-m. Geologically, it may be interpreted as Coarse sand and Medium sand with low moisture content together with the highly weathered portion of the bed rock. However, the resistivity of this horizon displayed the bottom of the layer around VES 15 and this resistivity response may be described as the weathered part of the Biotite Schist. The overall thickness of this layer varies from 40-50 m.

The bottom layer showing a resistivity range of 325-443 Ω-m is interpreted to be a Biotite Schist bed rock response. The depth to the fresh Biotite Schist is found to be relatively minimum around VES 14 and VES 16, and maximum around VES 15.

All the apparent resistivity distribution on the pseudo-section of profile three (Fig. 18) to some extent show a parallel pattern and inclined towards the Eastern side, which indicate horizontal homogenous distributions of each layer resistivity. The apparent resistivity along the vertical section exhibits a gradual increasing trend towards the upper section and towards the bottom section with the respect to a depth of AB/2 about (10-20) m. From the Western flank up to 650 E, the high resistivity zone > 70 Ω m on the top most portion of the section seems the response from the Slity clay soil which cover the upper part. Further down, the resistivity decreases < 40 Ω-m about AB/2 = 10 m which may be due to less saturated Sandy limestone, Sand and Gravel, and then the resistivity shows a continuous increment towards the bottom section, this may indicate the effect of the weathered and fresh bed rock. All the layers on the section seems deeper in the vicinity of 150 E and 300 E and becomes shallower towards the Eastern end.

Analysis of the geoelectric and pseudo-section has provided useful information regarding the thickness and depth ranges of each layers. The probable zone of the buried channel which contains the aquifer was clearly identified on the vertical section due to its resistivity behaviors. However, to see the subsurface lateral resistivity variation and to observe the extent and strike of the buried channel, the apparent resistivity maps for electrode positions of AB/2 = 45 m and 100 m were plotted Figs. 19 and 20. These electrode spreads were chosen because of the interest in the lateral variation and the structure of the acquifer which is identified on the geoelectric section.

Further, due to the east-west orientation of the profile lines and smallness of the surveyed area, the extent of the buried channel was not clearly located. If the orientation of the profile lines were perpendicular to the strike of the buried channel which is 58° NE of the surveyed area, as described by Moges Tigabe, the extent of the buried channel would be fully located. Nevertheless, to some degree, the suspected NW-SE trend of the buried channel is observed (Fig. 19 & 20).

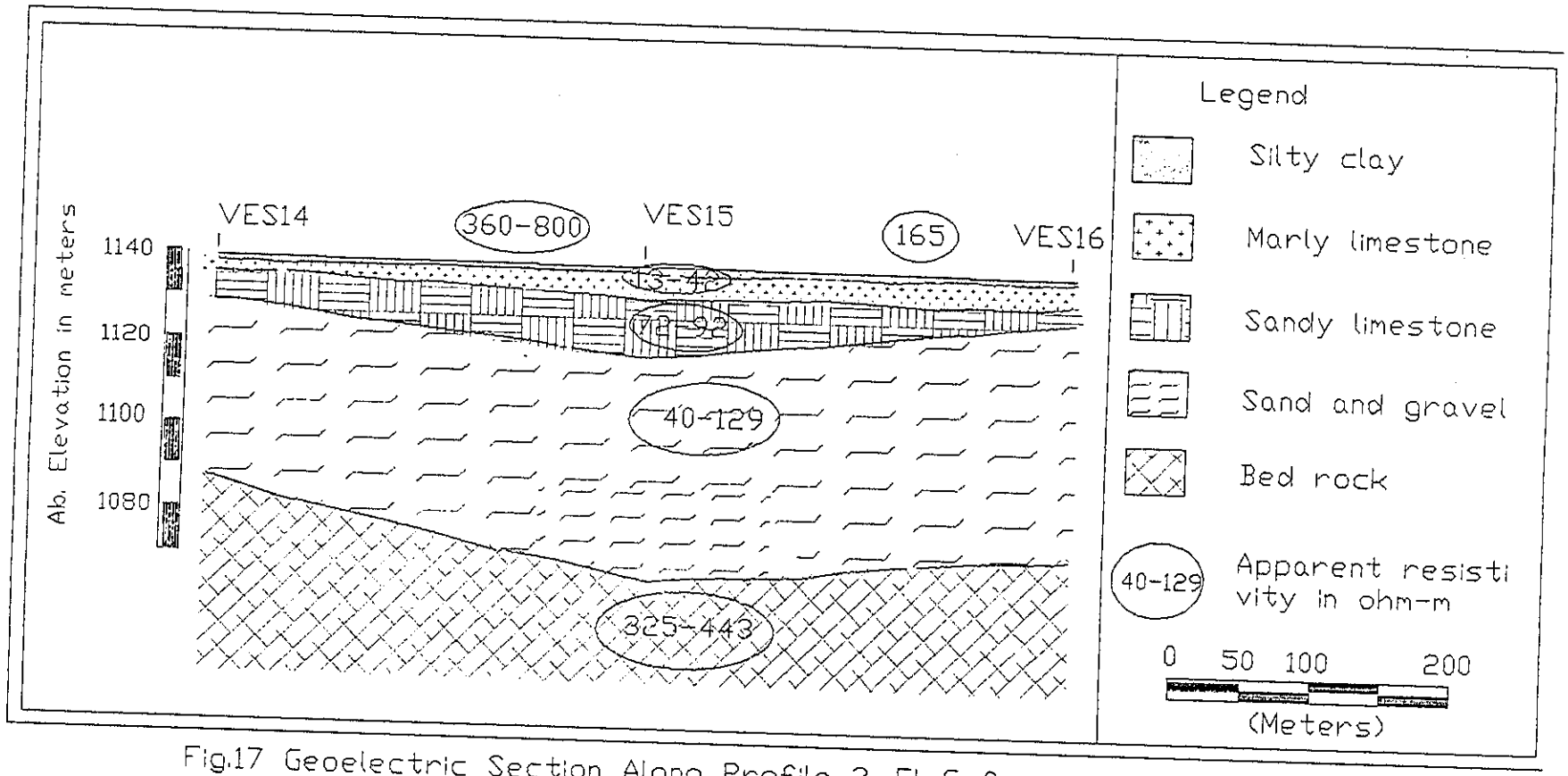

Fig.17 Geoelectric Section Along Profile 3, El-Gof.

Fig. 18 Apparent resistivity Pseudo-section of profile 3

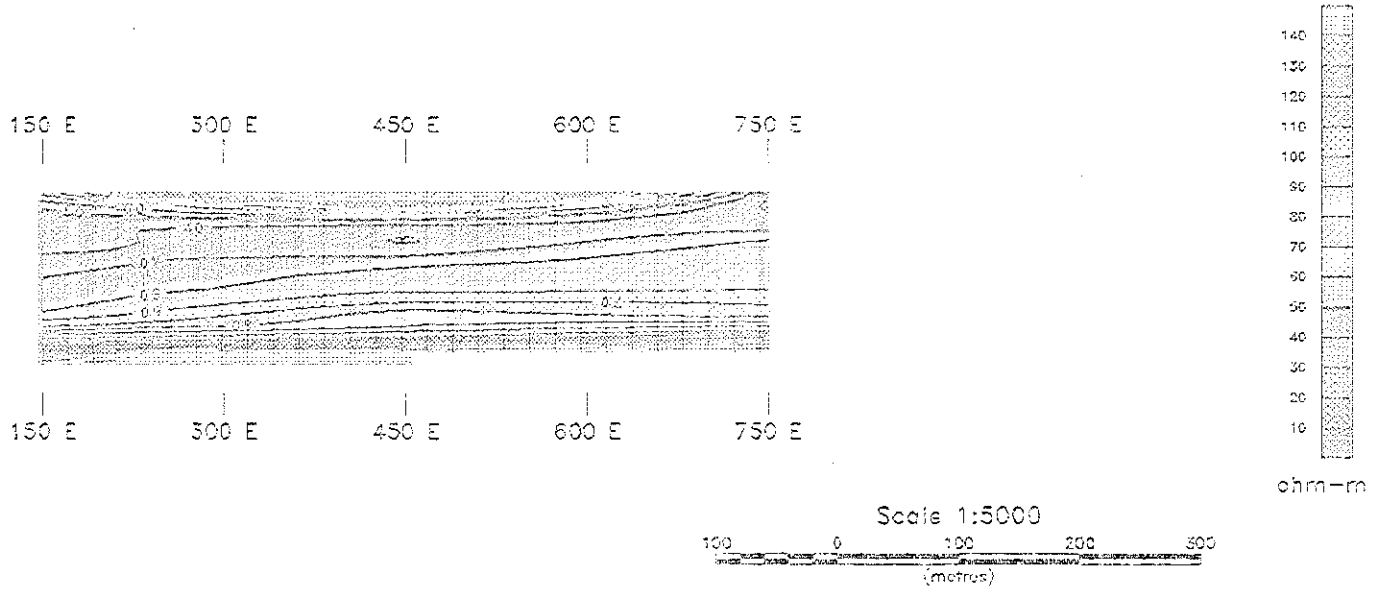

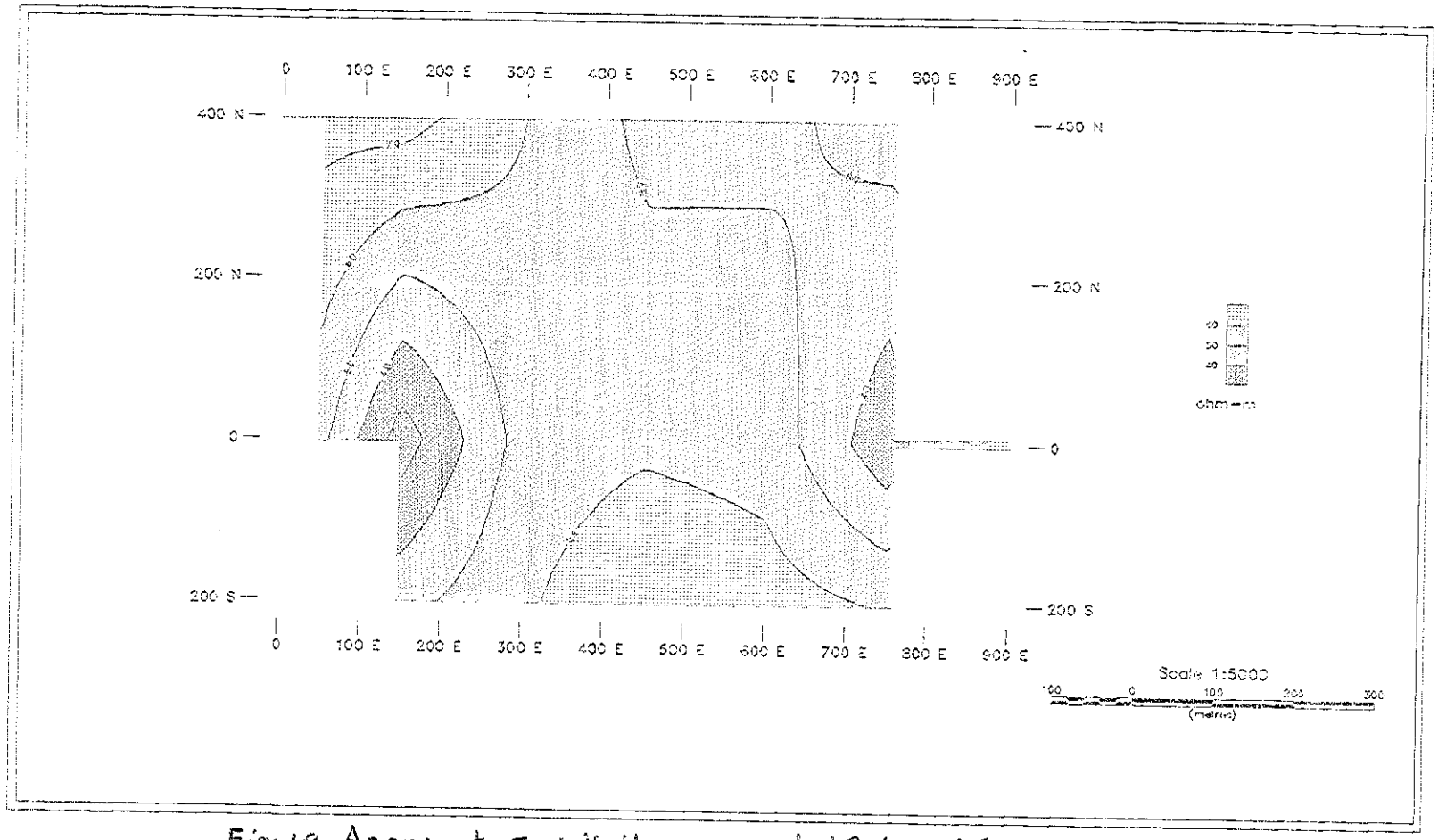

Fig. 19 Apparent resistivity map at AB/2 = 45 m

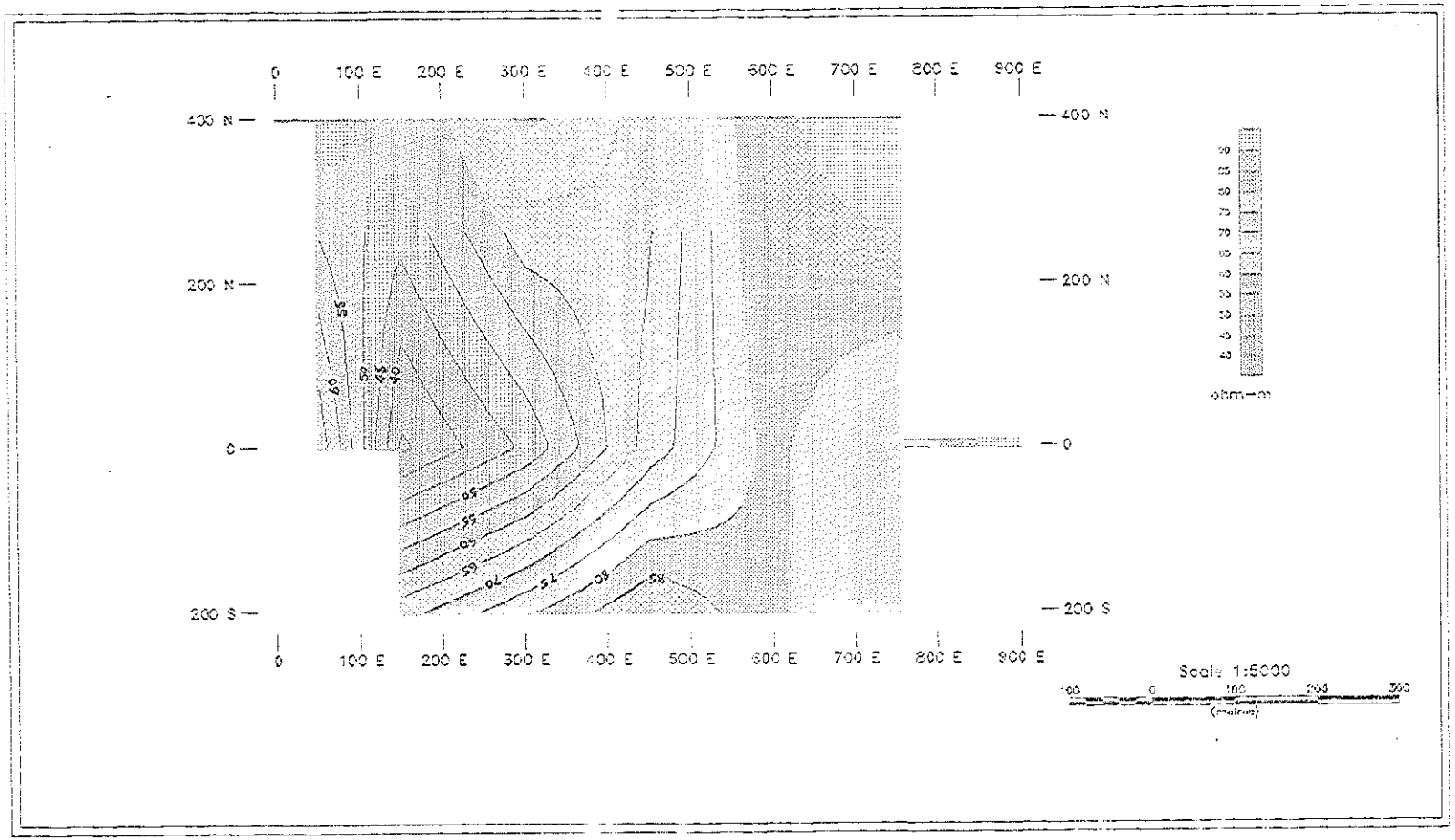

Fig. 26 Apparent resistivity map at AB/2 = 100 m, E0-E0f

The geoelectrical section of each profiles depicted lithologic variations and indicate on the average about five geoelectrical layers. Accordingly, the resistive layers with resistivity range from (17-52) ohm-m are sand and gravel deposits which are expected to be the likely host of water saturated sand and gravel deposits.

From the apparent resistivity map of AB/2 = 45 m and 100 m, low resistivity is observed in the SW & NE part of the survey area which is interpreted as being due to the buried river valley whereas the relatively highs in the NW & SE part may be attributed to shallow bedrock and possibly form barrier within the channel. This condition is also observed on the geoelectrical sections .

Thus, the result of the resistivity survey shows that the buried channel exhibits undulations (shallow and deep) along its course. This is evident from the undulating structures of the bed rock and the variations of the sand and gravel deposit in the area. Accordingly, the most favorable locations to site boreholes are within the resistivity lows, that is found in the SW & NE part of the survey area, as observed from the apparent resistivity map at AB/2 = 45 m. Thus these part of the area probably correspond to the deeper part of the buried channel and therefore are likely to contain thick succession of sand and gravel deposits.

The resistivity results were compared with the previous gravity results and it was found to be in a good agreement

Therefore, like the gravity method the resistivity method also play a major role for locating potential aquifers by delineating buried valleys.

5.4 Summary and Conclusion

The resistivity Sounding Surveys conducted along the three profile lines have enabled to delineate the buried river channel.

To achieve the objective of the Schlumberger resistivity survey, a total of 16 vertical electrical sounding stations where measured along three profile lines with electrode spacing (AB) ranging from 220-330 m. The following procedures have been followed to obtain the results.

1. All measured sounding data were plotted on logarithmic transparent paper of the same scale with the partial curve matching and auxiliary point method used in the interpretation.
2. All the data were corrected for the effect of the finite distance of MN spacing on resistivity values using the software program "SEV".
3. Using the depth/thickness and resistivity parameters acquired by iterative interpretation of sounding curves, the geoelectric section of each profiles were constructed by computer software. Moreover, the pseudo-section for each profiles and apparent resistivity maps for constant electrode spread positions of AB/2 = 45 m and 100 m were also constructed by using computer program(software).

Analysis of geoelectric section, pseudo section and apparent resistivity map at AB/2 = 45 m and 100 m has provided useful information regarding the thickness and depth larger of layers.

e. VES 5

$\frac{AB}{2}$	MN	K	ΔV(MV)	I (MA)
1.5	1.0	6.28	828	283
2.1	1.0	13.1	158	135
3.0	1.0	27.5	92.7	182
4.2	1.0	54.7	42	133
6.0	1.0	113	27.4	167
9.0	1.0	254	15.9	184
13.5	1.0	572	26.2	540
20	1.0	1250	4.08	150
20	12.0	95.3	64.5	145
30	1.0	2830	3.63	230
30	12.0	226	41.1	170
45	12.0	520	7.95	62
66	12.0	1130	5.7	78
100	12.0	2620	4.38	105
150	12.0	5880	3.87	157
150	90.0	715	28.2	161
220	12.0	12600	1.87	121
220	90.0	1620	12.9	124
330	90.0	3750	10.7	178

f. VES 6

$\frac{AB}{2}$	MN	K	ΔV(MV)	I (MA)
1.5	1.0	6.28	1206	123
2.1	1.0	13.1	444	130
3.0	1.0	27.5	161	120
4.2	1.0	54.7	96.6	154
6.0	1.0	113	30	110
9.0	1.0	254	16	134
13.5	1.0	572	8.19	128
20	1.0	1250	4.02	133
20	12.0	95.3	54.3	139
30	1.0	2830	1.81	118
30	12.0	226	20	105
45	12.0	520	9.66	97
66	12.0	1130	6.6	109
100	12.0	2620	11.5	319
150	12.0	5880	5.28	242
150	90.0	715	41.1	246
220	12.0	12600	2.44	171
220	90.0	1620	19	175

g. VES 7

$\frac{AB}{2}$	MN	K	ΔV(MV)	I (MA)
1.5	1.0	6.28	1680	72
2.1	1.0	13.1	690	95
3.0	1.0	27.5	195	70
4.2	1.0	54.7	113	85
6.0	1.0	113	85.8	99
9.0	1.0	254	96	114
13.5	1.0	572	13.1	140
20	1.0	1250	10.4	67
20	12.0	95.3	38.1	69
30	1.0	2830	3.96	172
30	12.0	226	36.9	140
45	12.0	520	9.3	90
66	12.0	1130	4.92	77
100	12.0	2620	3.18	117
150	12.0	5880	1.14	71
150	90.0	715	4.2	43
220	12.0	12600	1.27	113
220	90.0	1620	4.29	64
330	90.0	3750	2.83	61

h. VES 8

$\frac{AB}{2}$	MN	K	ΔV(MV)	I (MA)
1.5	1.0	6.28	1570	146
2.1	1.0	13.1	372	122
3.0	1.0	27.5	115	132
4.2	1.0	54.7	38.6	133
6.0	1.0	113	18	135
9.0	1.0	254	7.95	127
13.5	1.0	572	5.1	117
20	1.0	1250	45	130
20	12.0	95.3	1.55	153
30	1.0	2830	24.1	127
30	12.0	226	14.4	164
45	12.0	520	14.6	162
66	12.0	1130	2.79	450
100	12.0	2620	1.26	155
150	12.0	5880	11.1	124
150	90.0	715	1.05	118
220	12.0	12600	8.4	135
220	90.0	1620	4.86	133

APPENDIX A
ROW FIELD DATA

a. VES 1

$\frac{AB}{2}$	MN	K	ΔV(MV)	I (MA)
1.5	1.0	6.28	2060	162
2.1	1.0	13.1	747	1670
3.0	1.0	27.5	441	259
4.2	1.0	54.7	247	263
6.0	1.0	113	164	291
9.0	1.0	254	72.9	223
13.5	1.0	572	48.3	270
20	1.0	1250	16.5	203
20	12.0	95.3	202	211
30	1.0	2830	4.47	142
30	12.0	226	63	173
45	12.0	520	33.3	246
66	12.0	1130	7.74	203
100	12.0	2620	2.08	140
150	12.0	5880	1.33	133
150	90.0	715	6.24	101
220	12.0	12600	15.5	480
220	90.0	1620	4.62	298
330	90.0	3750	14.3	133

b. VES 2

$\frac{AB}{2}$	MN	K	ΔV(MV)	I (MA)
1.5	1.0	6.28	2930	453
2.1	1.0	13.1	870	337
3.0	1.0	27.5	348	294
4.2	1.0	54.7	189	309
6.0	1.0	113	77.7	236
9.0	1.0	254	20.2	121
13.5	1.0	572	42.9	475
20	1.0	1250	15	326
20	12.0	95.3	14.1	334
30	1.0	2830	10.6	436
30	12.0	226	92.4	440
45	12.0	520	14	145
66	12.0	1130	7.41	200
100	12.0	2620	1.52	107
150	12.0	5880	1.26	139
150	90.0	715	4.83	67
220	12.0	12600	1.92	301
220	90.0	1620	13.8	287
330	90.0	3750	4.89	161

c. VES 3

$\frac{AB}{2}$	MN	K	ΔV(MV)	I (MA)
1.5	1.0	6.28	5160	119
2.1	1.0	13.1	549	143
3.0	1.0	27.5	58.5	69
4.2	1.0	54.7	27.5	77
6.0	1.0	113	22.2	112
9.0	1.0	254	11.1	100
13.5	1.0	572	8.73	144
20	1.0	1250	17.1	505
20	12.0	95.3	187	511
30	1.0	2830	3.21	175
30	12.0	226	33.1	163
45	12.0	520	20.5	210
66	12.0	1130	5.28	124
100	12.0	2620	5.9	368
150	12.0	5880	2.44	230
150	90.0	715	22	221
220	12.0	12600	1.14	58
220	90.0	1620	7.89	125
330	90.0	3750	16.2	80

d. VES 4

$\frac{AB}{2}$	MN	K	ΔV(MV)	I (MA)
1.5	1.0	6.28	2280	109
2.1	1.0	13.1	513	90
3.0	1.0	27.5	119	78
4.2	1.0	54.7	26.4	54
6.0	1.0	113	14.2	62
9.0	1.0	254	10.72	124
13.5	1.0	572	12.5	242
20	1.0	1250	3.96	144
20	12.0	95.3	72.9	125
30	1.0	2830	3.6	242
30	12.0	226	74.7	245
45	12.0	520	47.7	335
66	12.0	1130	5.13	65
100	12.0	2620	8.7	233
150	12.0	5880	3.06	131
150	90.0	715	25.1	130
220	12.0	12600	2.09	140
220	90.0	1620	17.8	143
330	90.0	3750	8.58	110

i. VES 9

$\frac{AB}{2}$	MN	K	ΔV(MV)	I (MA)
1.5	1.0	6.28	4100	522
2.1	1.0	13.1	100	124
3.0	1.0	27.5	167	170
4.2	1.0	54.7	48.6	91
6.0	1.0	113	22.5	62
9.0	1.0	254	13	61
13.5	1.0	572	26.8	246
20	1.0	1250	5.01	114
20	12.0	95.3	62.7	112
30	1.0	2830	2.74	111
30	12.0	226	11.4	35
45	12.0	520	21.3	202
66	12.0	1130	3.21	65
100	12.0	2620	2.58	128
150	12.0	5880	1.68	48
150	90.0	715	17.4	176
220	12.0	12600	1.25	160
220	90.0	1620	9.84	156
330	90.0	3750	15	345

j. VES 10

$\frac{AB}{2}$	MN	K	ΔV(MV)	I (MA)
1.5	1.0	6.28	16200	100
2.1	1.0	13.1	6870	159
3.0	1.0	27.5	1670	110
4.2	1.0	54.7	282	99
6.0	1.0	113	54.9	115
9.0	1.0	254	9.48	62
13.5	1.0	572	8.28	114
20	1.0	1250	12.0	314
20	12.0	95.3	107.4	256
30	1.0	2830	3.87	193
30	12.0	226	39	194
45	12.0	520	5.7	61
66	12.0	1130	8.1	167
100	12.0	2620	12.6	470
150	12.0	5880	1.81	137
150	90.0	715	16.7	167
220	12.0	12600	1.17	122
220	90.0	1620	6.15	84
330	90.0	3750	7.14	168

k. VES 11

$\frac{AB}{2}$	MN	K	ΔV(MV)	I (MA)
1.5	1.0	6.28	16700	153
2.1	1.0	13.1	6930	149
3.0	1.0	27.5	2640	137
4.2	1.0	54.7	909	105
6.0	1.0	113	345	140
9.0	1.0	254	131	198
13.5	1.0	572	26.4	149
20	1.0	1250	20	325
20	12.0	95.3	274	326
30	1.0	2830	3.72	183
30	12.0	226	45.6	179
45	12.0	520	18.7	159
66	12.0	1130	17.1	275
100	12.0	2620	4.71	140
150	12.0	5880	3.78	217
150	90.0	715	24.1	219
220	12.0	12600	3.9	326
220	90.0	1620	23.6	323
330	90.0	3750	10.7	233

l. VES 12

$\frac{AB}{2}$	MN	K	ΔV(MV)	I (MA)
1.5	1.0	6.28	3030	175
2.1	1.0	13.1	912	177
3.0	1.0	27.5	393	142
4.2	1.0	54.7	279	238
6.0	1.0	113	83.4	196
9.0	1.0	254	29	224
13.5	1.0	572	15.6	270
20	1.0	1250	3	137
20	12.0	95.3	35.4	268
30	1.0	2830	3.15	270
30	12.0	226	34.2	450
45	12.0	520	23.7	290
66	12.0	1130	9.45	163
100	12.0	2620	3.36	191
150	12.0	5880	2.24	153
150	90.0	715	19.4	150
220	12.0	12600	6.75	152
220	90.0	1620	12.1	102
330	90.0	3750	3.63	125

m. VES 13

$\frac{AB}{2}$	MN	K	ΔV(MV)	I (MA)
1.5	1.0	6.28	1100	230
2.1	1.0	13.1	292	123
3.0	1.0	27.5	381	315
4.2	1.0	54.7	133	191
6.0	1.0	113	143	347
9.0	1.0	254	42	175
13.5	1.0	572	26	209
20	1.0	1250	8.82	155
20	12.0	95.3	92.1	148
30	1.0	2830	2.63	107
30	12.0	226	17	60
45	12.0	520	51.3	413
66	12.0	1130	13.3	212
100	12.0	2620	25.8	767
150	12.0	5880	3.08	144
150	90.0	715	29.1	185
220	12.0	12600	3.57	278
220	90.0	1620	27.2	275
330	90.0	3750	10.9	190

n. VES 14

$\frac{AB}{2}$	MN	K	ΔV(MV)	I (MA)
1.5	1.0	6.28	2160	189
2.1	1.0	13.1	555	143
3.0	1.0	27.5	384	229
4.2	1.0	54.7	161	183
6.0	1.0	113	65.7	165
9.0	1.0	254	45	279
13.5	1.0	572	5.79	91
20	1.0	1250	4.98	154
20	12.0	95.3	46.8	117
30	1.0	2830	3.06	197
30	12.0	226	38.6	200
45	12.0	520	17.3	203
66	12.0	1130	12.5	291
100	12.0	2620	3.93	155
150	12.0	5880	2.55	160
150	90.0	715	19	162
220	12.0	12600	1.11	114
220	90.0	1620	3.09	50

o. VES 15

$\frac{AB}{2}$	MN	K	ΔV(MV)	I (MA)
1.5	1.0	6.28	4140	117
2.1	1.0	13.1	909	118
3.0	1.0	27.5	204	103
4.2	1.0	54.7	113	198
6.0	1.0	113	30	115
9.0	1.0	254	10.5	73
13.5	1.0	572	7.6	90
20	1.0	1250	5.1	115
20	12.0	95.3	60.3	119
30	1.0	2830	5.1	74
30	12.0	226	1.5	75
45	12.0	520	16.9	209
66	12.0	1130	24.4	75
100	12.0	2620	5.4	266
150	12.0	5880	7.05	77
150	90.0	715	1.25	74
220	12.0	12600	8.31	130
220	90.0	1620	1.28	128

p. VES 16

$\frac{AB}{2}$	MN	K	ΔV(MV)	I (MA)
1.5	1.0	6.28	1540	228
2.1	1.0	13.1	603	251
3.0	1.0	27.5	157	150
4.2	1.0	54.7	80.4	142
6.0	1.0	113	54.3	155
9.0	1.0	254	33.0	165
13.5	1.0	572	18.6	185
20	1.0	1250	8.1	175
20	12.0	95.3	63.3	140
30	1.0	2830	4.2	201
30	12.0	226	36.0	188
45	12.0	520	18.0	220
66	12.0	1130	5.1	82
100	12.0	2620	2.4	117
150	12.0	5880	2.6	211
150	90.0	715	19.1	191
220	12.0	12600	1.2	156
220	90.0	1620	8.7	150

APPENDIX B

Results of one - dimensional model interpretation of the Schlumberger resistivity sounding measurements

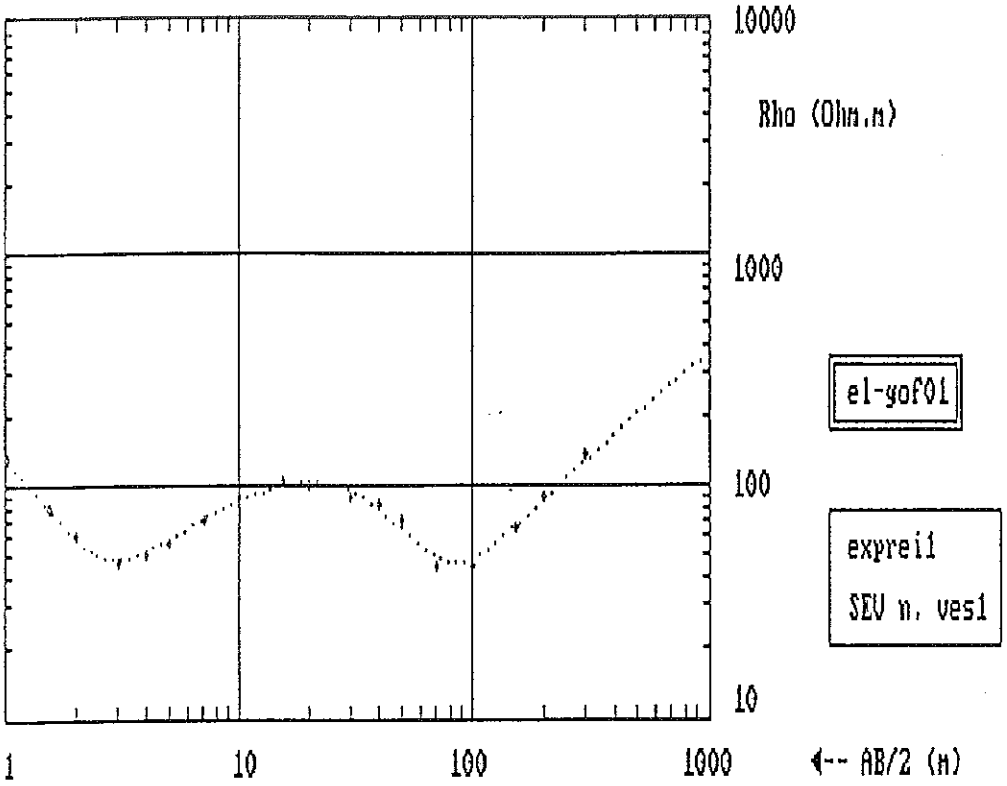
10000
Rho (Ohm.m)
1000
el-gof01
100
expreil
SEV n. vesl
10
1
10
100
1000
<-- AB/2 (m)

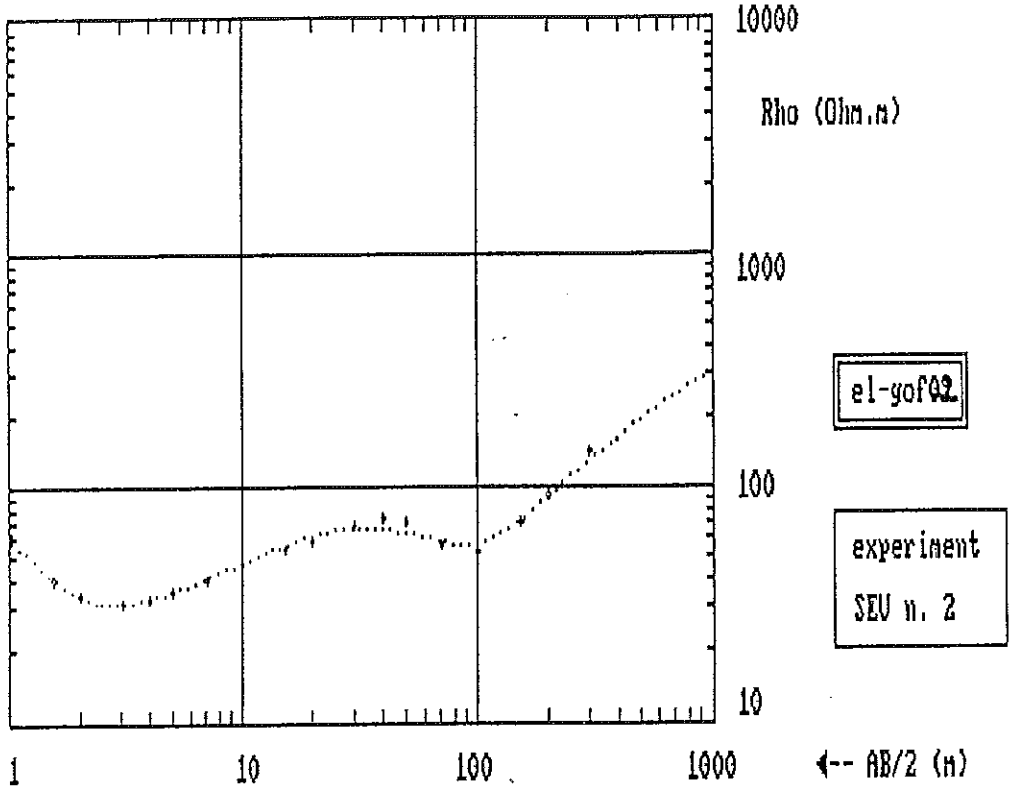
10000
Rho (Ohm.m)
1000
el-gof02
100
experiment
SEU n. 2
10
1
10
100
1000
<-- AB/2 (m)

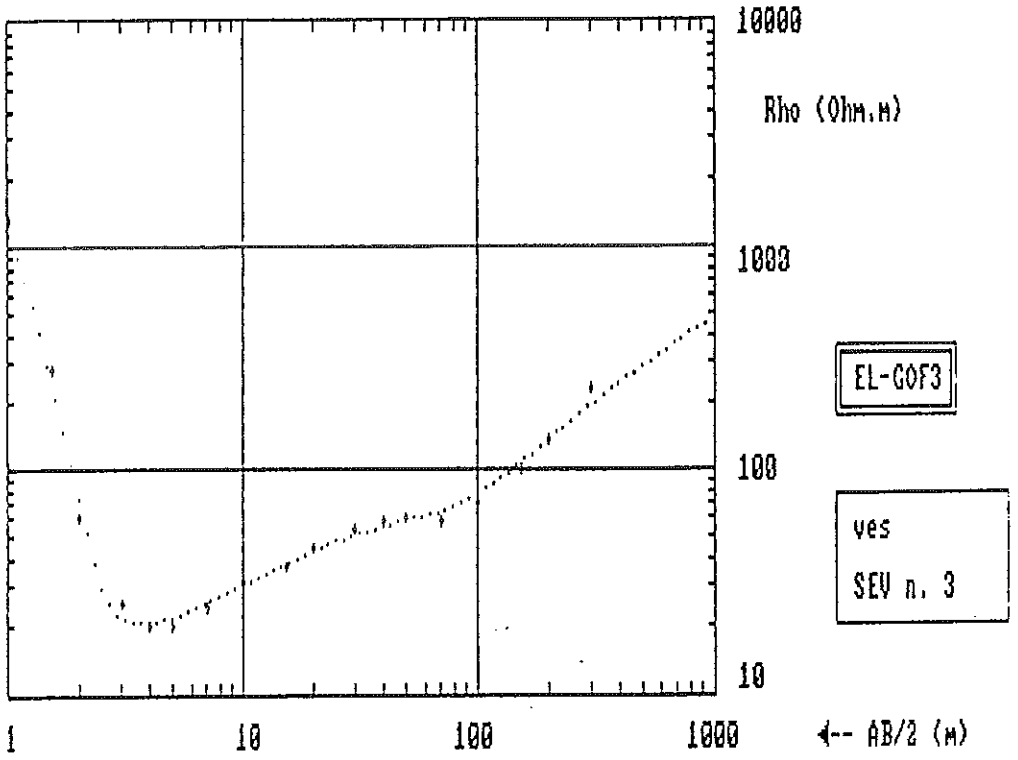

LAYER No.	RESISTIVITY (Ohm-m)	THICNESS (m)	DEPTH FROM THE TOP SURFACE (m)
1	4734.79	0.38	0.00
2	22.07	1.38	-0.38
3	11.14	1.23	-1.76
4	44.81	3.25	-2.99
5	49.25	4.13	-6.24
6	103.51	8.34	-10.37
7	65.31	8.54	-18.71
8	23.42	18.11	-27.26
9	1096.68	∞	-45.36

Standard deviation = 0.08
Max relative error = -0.18 at AB/2 = 316
No. of iteration = 50

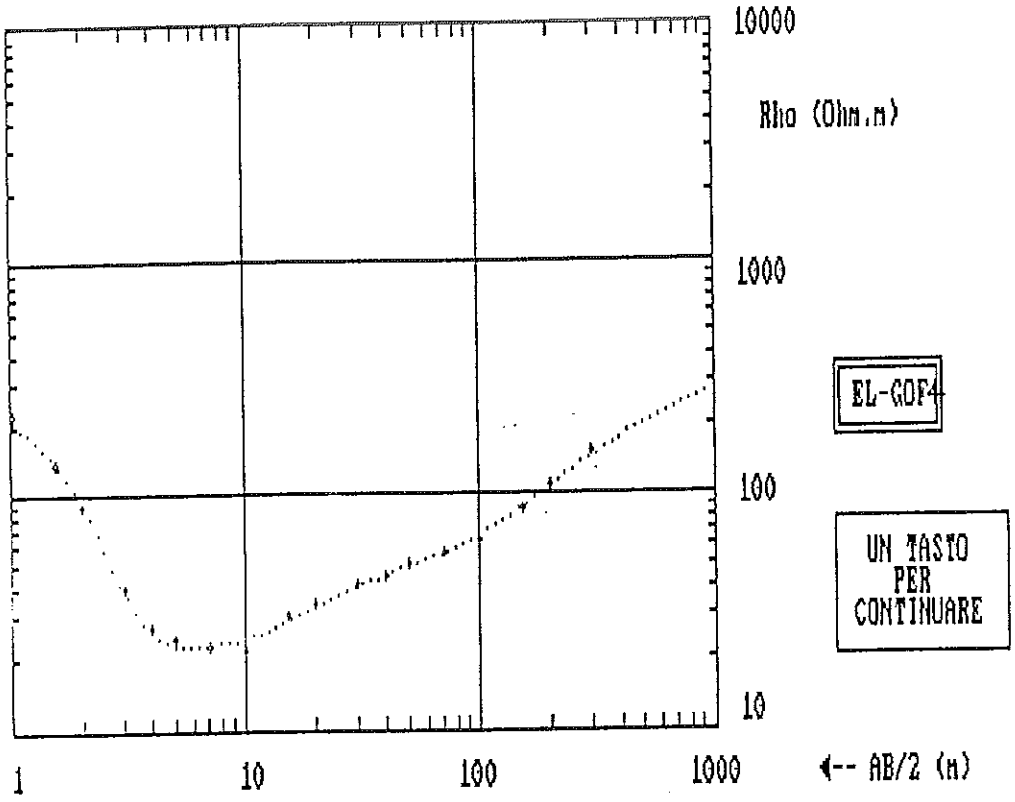

LAYER No.	RESISTIVITY (Ohm-m)	THICNESS (m)	DEPTH FROM THE TOP SURFACE (m)
1	270.46	0.76	0.00
2	41.27	0.31	-0.76
3	15.59	1.38	-1.07
4	28.38	1.93	-2.45
5	10.09	2.29	-4.38
6	125.28	3.35	-6.67
7	52.66	55.92	-10.02
8	412.25	∞	-65.94

Standard deviation = 0.04

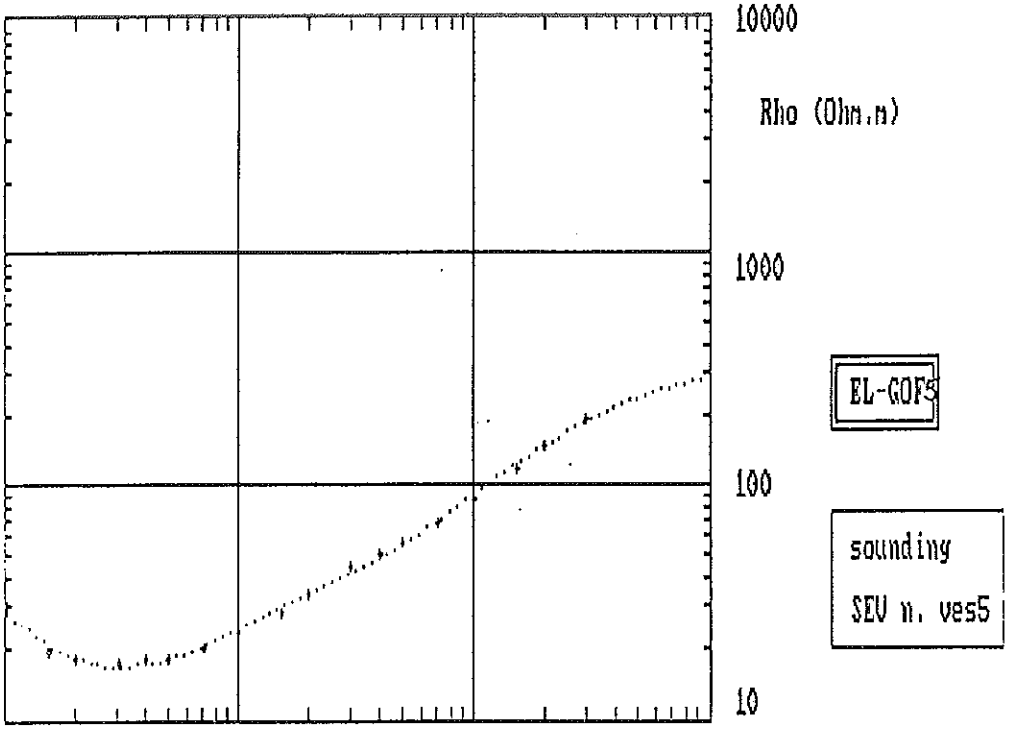

LAYER No.	RESISTIVITY (Ohm-m)	THICNESS (m)	DEPTH FROM THE TOP SURFACE (m)
1	46.50	0.43	0.00
2	14.83	1.73	-0.43
3	16.10	2.63	-2.16
4	50.61	29.71	-4.79
5	342.60	∞	-34.50

Standard deviation = 0.39
Max relative error = -0.07 at AB/2 = 31.6
No. of iteration = 33
Accepted deviation = 0.04

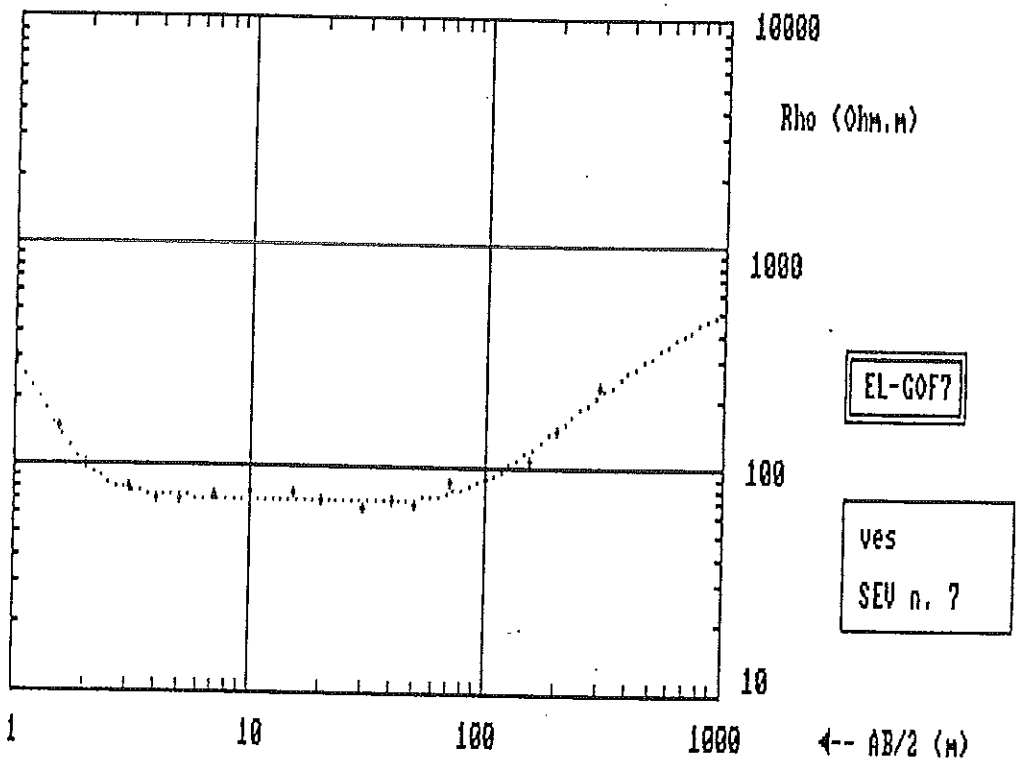

LAYER No.	RESISTIVITY (Ohm-m)	THICNESS (m)	DEPTH FROM THE TOP SURFACE (m)
1	641.28	0.44	0.00
2	70.85	17.13	-0.44
3	66.33	63.02	-17.58
4	1139.61	∞	-80.60

Standard deviation	= 0.05	
Max relative error	= -0.09	at AB/2 = 79.4
No. of iteration	= 8	
Accepted deviation	= 0.03	

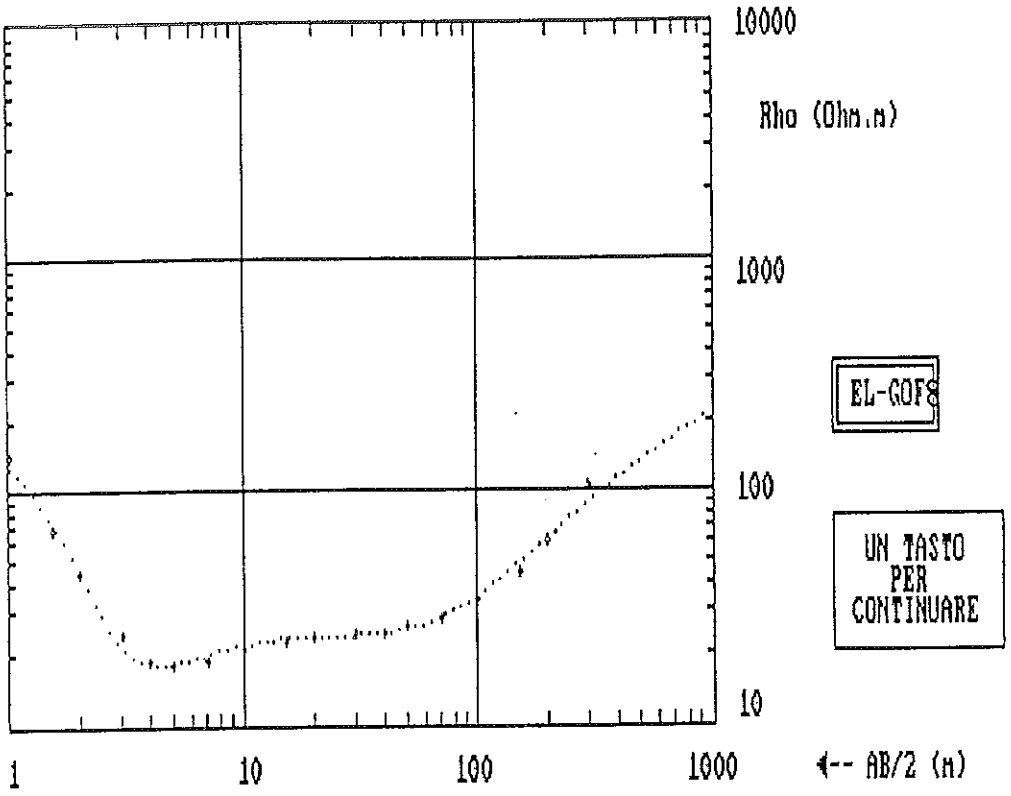
10000
Rho (Ohm.m)
1000
EL-GOF
100
UN TASTO
PER
CONTINUARE
10
1
10
100
1000
<-- AB/2 (m)

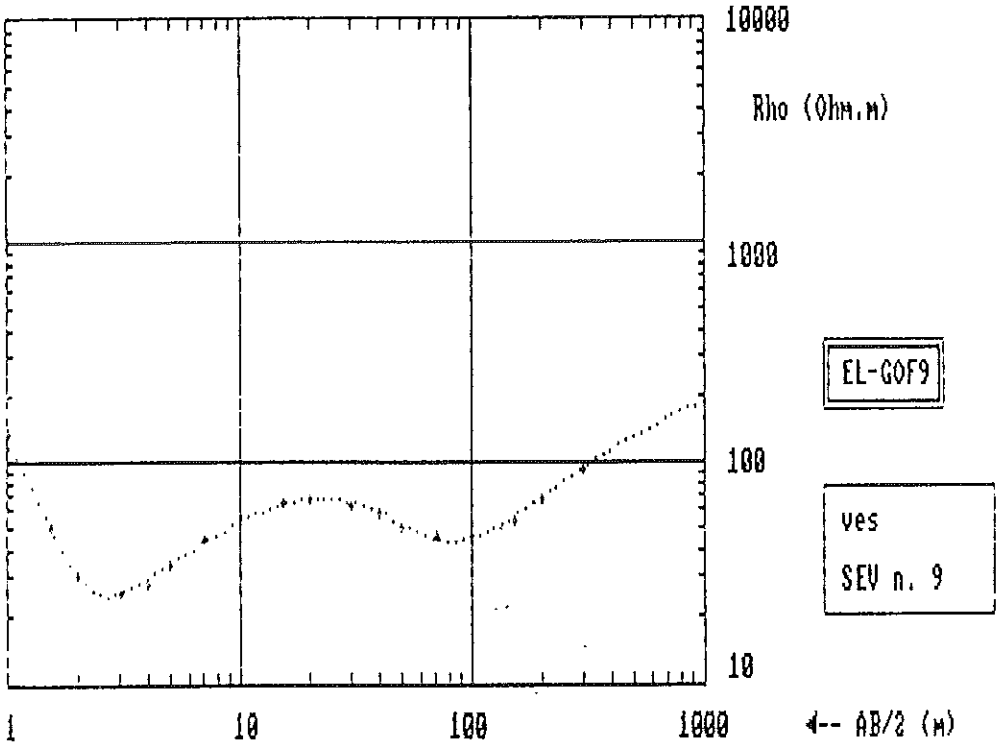

LAYER No.	RESISTIVITY (Ohm-m)	THICNESS (m)	DEPTH FROM THE TOP SURFACE (m)
1	276.03	0.47	0.00
2	12.51	0.81	-0.47
3	16.58	0.63	-1.28
4	97.20	2.31	-1.91
5	119.39	10.44	-4.22
6	20.63	24.67	-14.67
7	42.70	38.99	-39.34
8	280.00	∞	-78.33

Standard deviation = 0.04
Max relative error = -0.12 at AB/2 = 1
No. of iteration = 9
Accepted deviation = 0.03

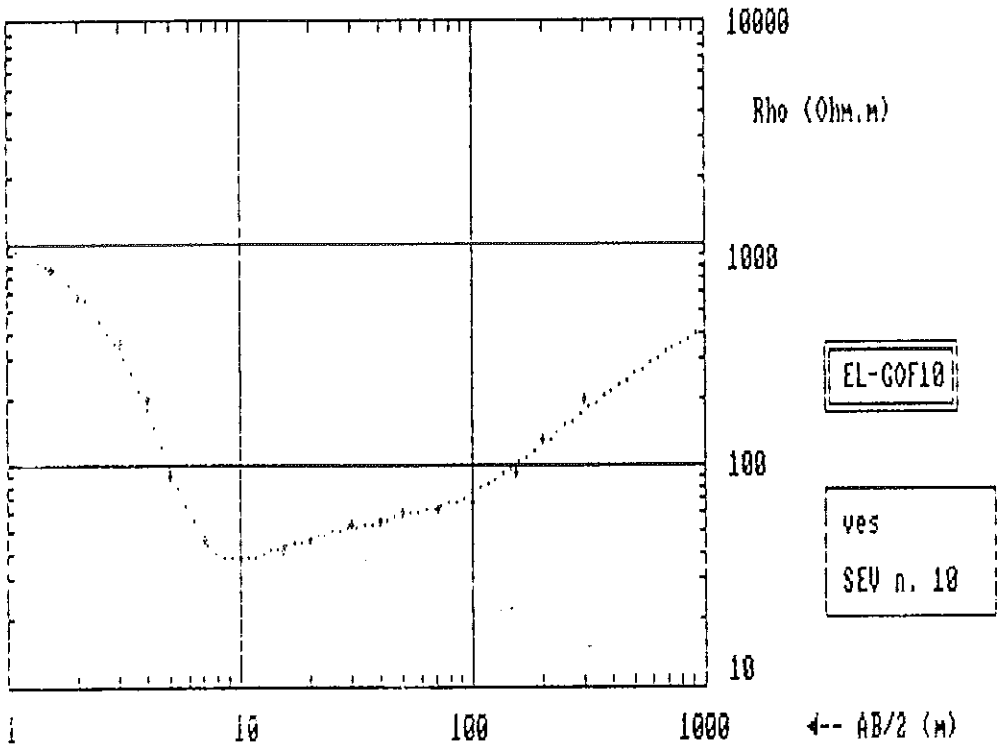

LAYER No.	RESISTIVITY (Ohm-m)	THICKNESS (m)	DEPTH FROM THE TOP SURFACE (m)
1	1083.66	0.93	0.00
2	335.49	0.91	-0.93
3	26.18	4.67	-1.84
4	62.60	23.99	-6.51
5	54.73	46.75	-30.50
6	845.21	∞	-77.26

Standared devation = 0.06
Max. relative error = -0.13
No. of iteration = 3

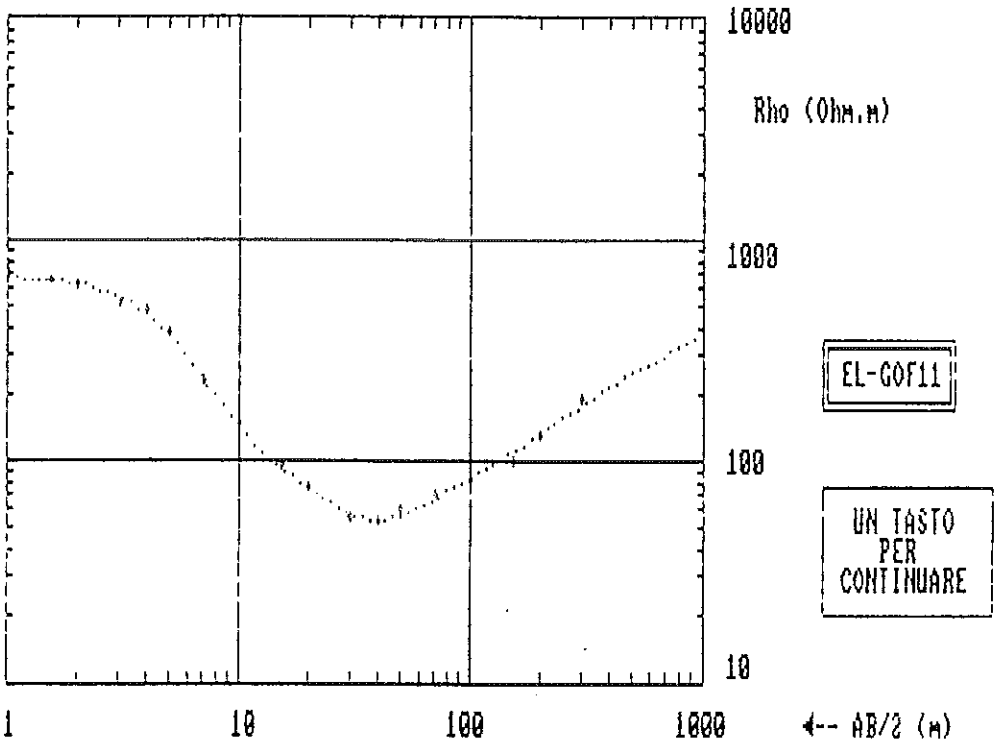

LAYER No.	RESISTIVITY (Ohm-m)	THICNESS (m)	DEPTH FROM THE TOP SURFACE (m)
1	678.72	2.47	0.00
2	98.43	10.00	-2.47
3	26.91	14.30	-12.47
4	115.86	27.99	-26.77
5	127.40	53.26	-54.75
6	569.96	∞	-100.00

Standard deviation = 0.04
Max relative error = -0.09 at AB/2 = 158.5
No. of iteration = 9
Accepted deviation = 0.03

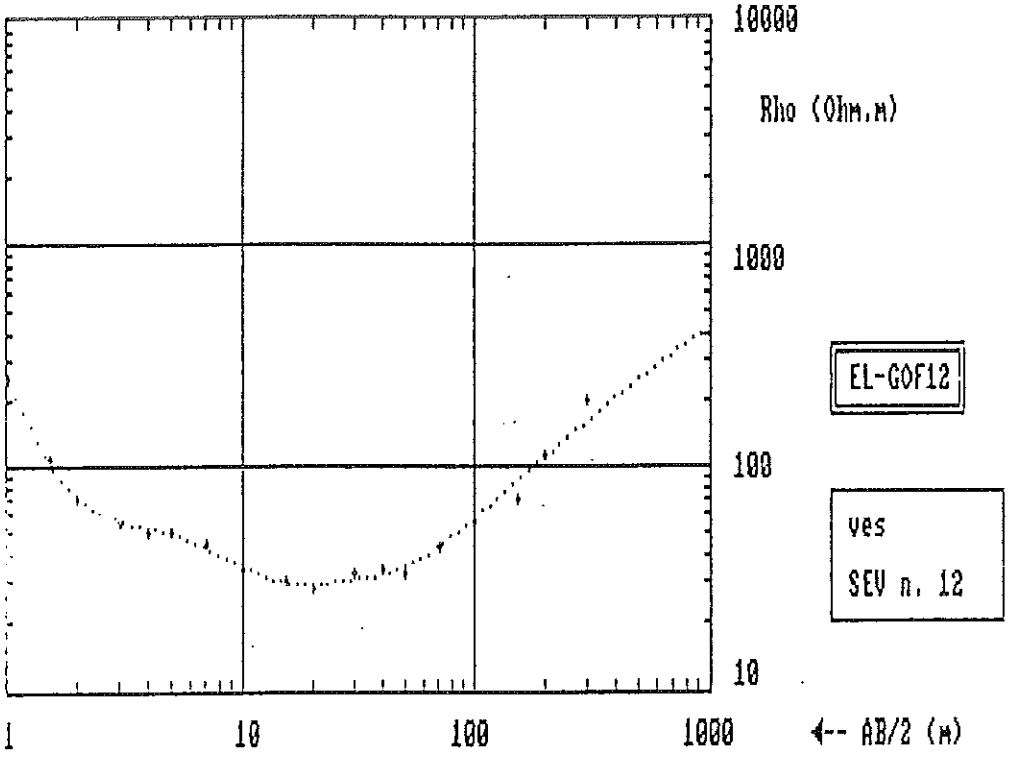
10000
Rho (Ohm.m)
1000
EL-GOF12
100
yes
SEV n. 12
10
1
10
100
1000
<-- AB/2 (m)

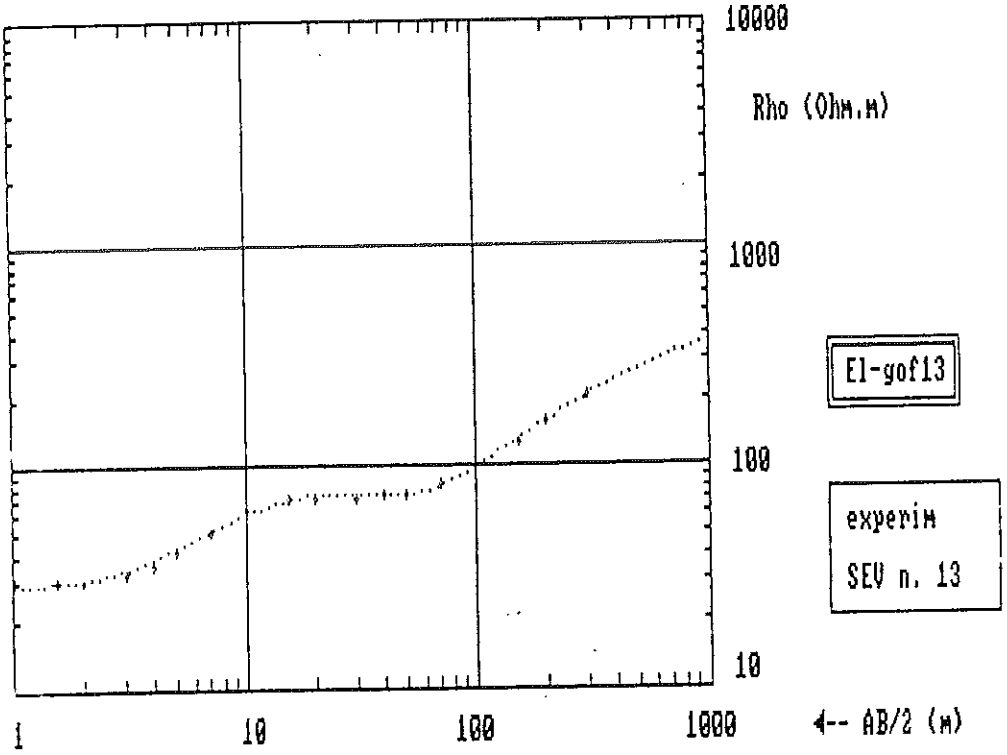

LAYER No.	RESISTIVITY (Ohm-m)	THICNESS (m)	DEPTH FROM THE TOP SURFACE (m)
1	29.00	1.90	0.00
2	39.31	0.73	-1.90
3	64.86	1.37	-2.63
4	164.31	2.76	-4.00
5	96.28	3.58	-6.76
6	50.35	23.73	-10.34
7	116.81	33.70	-34.07
8	454.30	∞	-67.77

Standard deviation = 0.027
Max relative error = -0.05 at AB/2 = 10.0
No. of iteration = 40
Accepted deviation = 0.03

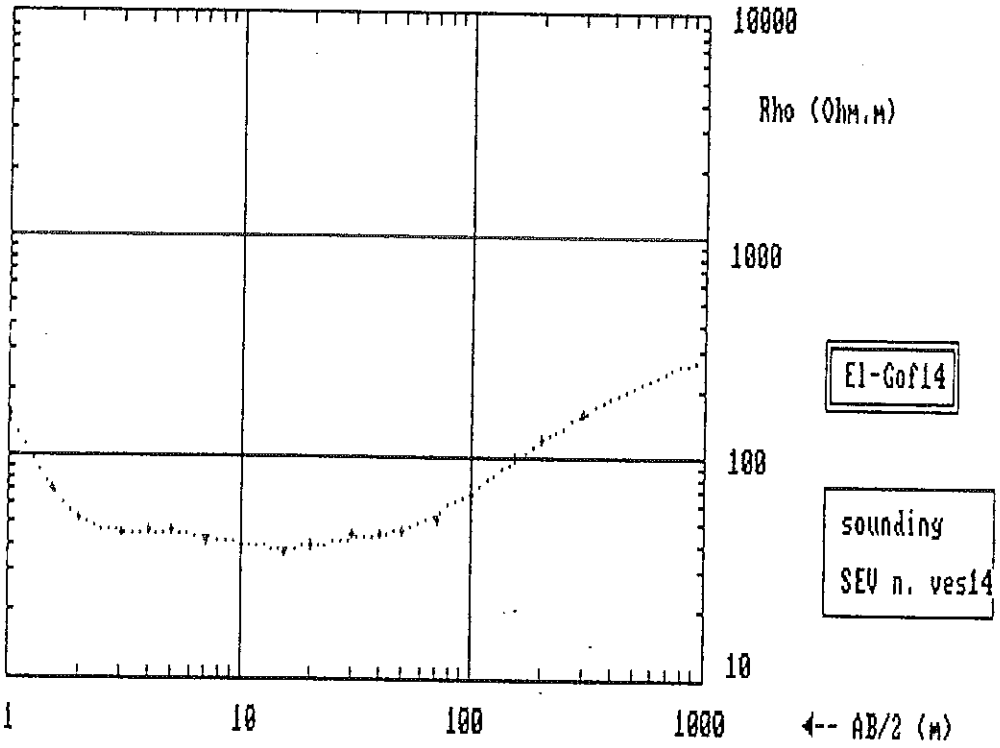

LAYER No.	RESISTIVITY (Ohm-m)	THICKNESS (m)	DEPTH FROM THE TOP SURFACE (m)
1	355.32	0.41	0.00
2	36.67	1.34	-0.41
3	74.24	1.04	-1.75
4	32.76	7.20	-2.79
5	48.11	7.77	-9.98
6	40.81	33.19	-17.76
7	368.84	∞	-50.95

Standared devation = 0.029
Max. relative error = -0.05
No. of iteration = 32

DDD D

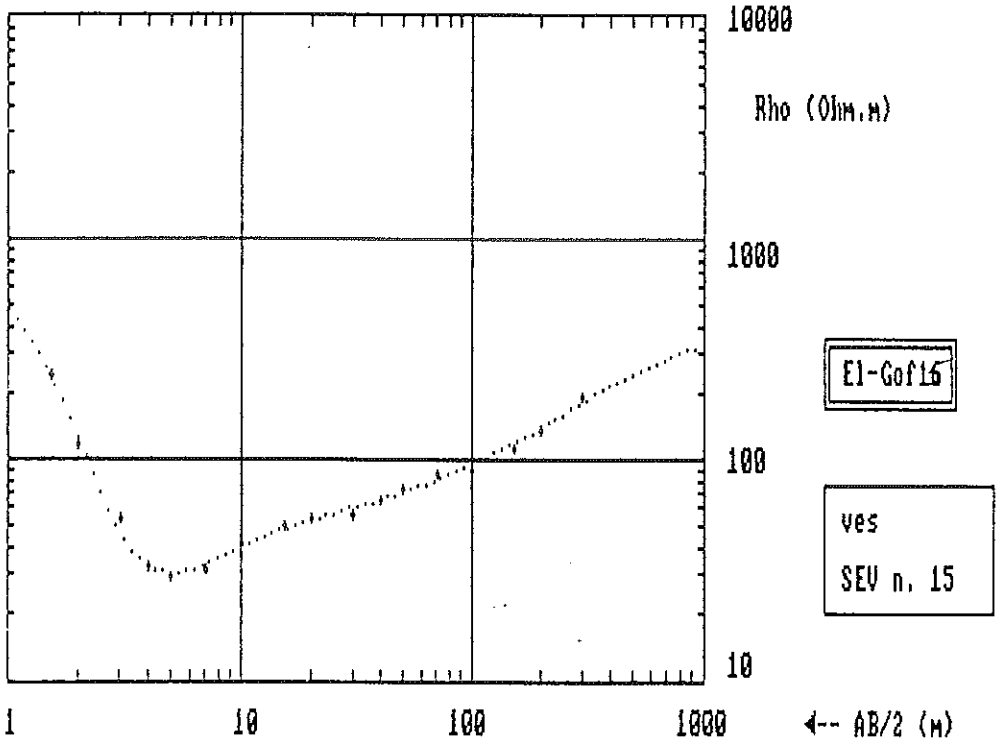

LAYER No.	RESISTIVITY (Ohm-m)	THICNESS (m)	DEPTH FROM THE TOP SURFACE (m)
1	821.71	0.58	0.00
2	42.99	1.35	-0.58
3	12.06	1.38	-1.93
4	84.25	3.84	-3.31
5	73.22	4.32	-7.15
6	46.13	9.90	-11.47
7	129.34	28.33	-21.37
8	56.10	24.37	-49.70
9	443.21	∞	-74.08

Standard deviation = 0.05
Max relative error = -0.1 at AB/2 = 3.2
No. of iteration = 5
Accepted deviation = 0.03

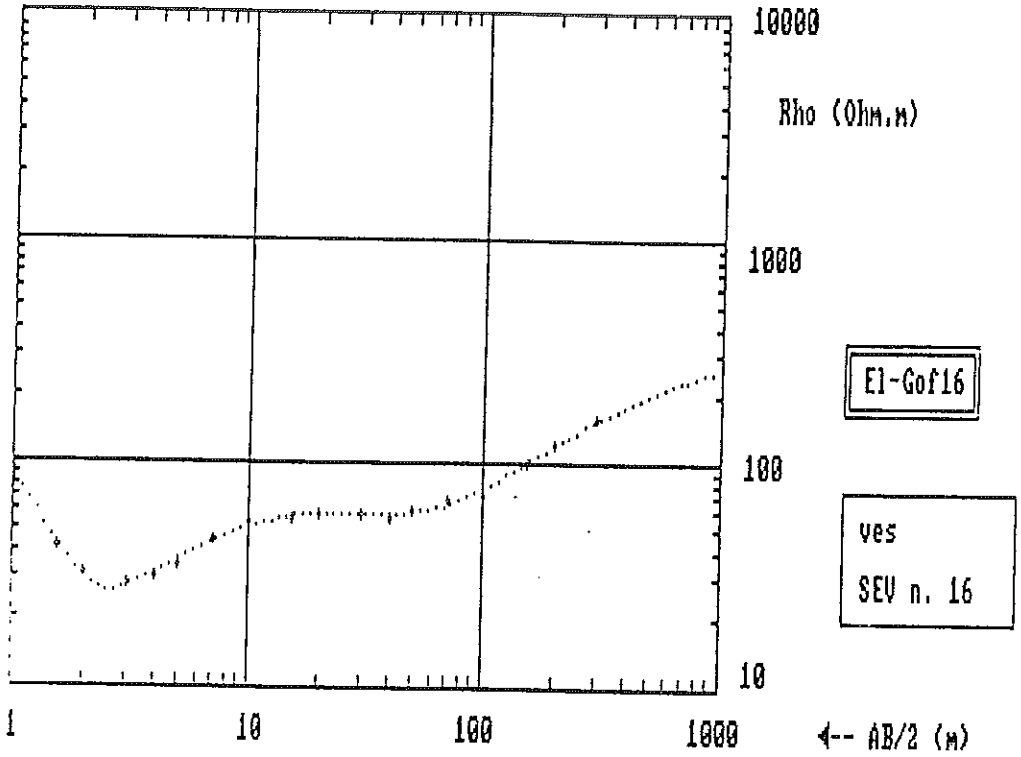

LAYER No.	RESISTIVITY (Ohm-m)	THICNESS (m)	DEPTH FROM THE TOP (m)
1	164.50	0.50	0.00
2	13.62	1.20	-0.50
3	92.58	4.35	-1.71
4	59.05	13.82	-6.05
5	27.45	7.11	-19.87
6	70.53	39.57	-26.98
7	325.01	∞	-66.56

Standard deviation = 0.046
Max relative error = -0.780 at AB/2 = 2.5
No. of iteration = 20
Accepted deviation = 0.03

LAYER No.	RESISTIVITY (Ohm-m)	THICNESS (m)	DEPTH FROM THE TOP SURFACE (m)
1	4734.79	0.38	0.00
2	22.07	1.38	-0.38
3	11.14	1.23	-1.76
4	44.81	3.25	-2.99
5	49.25	4.13	-6.24
6	103.51	8.34	-10.37
7	65.31	8.54	-18.71
8	23.42	18.11	-27.26
9	1096.68	∞	-45.36

Standard deviation = 0.08
Max relative error = -0.18 at AB/2 = 316
No. of iteration = 50
Accepted deviation = 0.04

LIMIT OF EQUIVALENCE (max. error = 5%)

Layer	$h_{min.}$	$h_{max.}$	ρ_{min}	ρ_{max}
1	0.37	0.38	4671.44	4801.79
2	1.20	1.55	19.65	25.36
3	0.7	1.62	6.32	14.62
4	2.5	3.95	34.52	54.44
5	1.85	5.69	22.03	67.84
6	4.36	11.23	76.89	197.98
7	5.87	10.75	51.93	95.03
8	0.00	35.87	0.00	46.39
9			777.34	1732.87

LAYER No.	RESISTIVITY (Ohm-m)	THICNESS (m)	DEPTH FROM THE TOP SURFACE (m)
1	184.19	0.66	0.00
2	13.33	2.51	-0.66
3	38.30	1.29	-3.17
4	23.35	2.04	-4.46
5	27.14	4.10	-6.50
6	20.53	11.20	-10.59
7	24.62	42.32	-21.79
8	97.04	13.33	-64.11
9	482.68	∞	-77.44

Standard deviation = 0.06
Max relative error = -0.17 at AB/2 = 316.2
No. of iteration = 10
Accepted deviation = 0.03

LIMIT OF EQUIVALENCE (max. error = 5%)

Layer	$h_{min.}$	$h_{max.}$	ρ_{min}	ρ_{max}
1	0.64	0.69	176.21	189.08
2	2.32	2.80	12.13	14.65
3	0.52	1.78	27.07	93.02
4	1.35	2.58	15.10	28.99
5	2.95	5.07	21.74	37.22
6	9.21	12.96	16.98	23.90
7	33.83	50.53	19.52	29.16
8	0.00	77.21	0.01	562.32
9			343.95	791.17

REFERENCES

Bekele Dewans, Getahun Kebede and Tsega Teklu, 1988. Hydrogeology & lower Dawa and Sure river basins, Sidamo, Ethiopia.

Carpenter, E.W. and Habberjam, G.M., 1956 a tri-potential method of resistivity prospecting Geophysics, V.21, p.455-469.

Coppock, D.L. (ed). 1994. The Borana Plateau of Southern Ethiopia: Synthesis of pastoral research, development and change, 1980-1991. ILCA, Addis Ababa Ethiopia. 393 pp.

Edward, L.S., 1977. A modified pseudosection for resistivity and IP. Geophysics, V. 42, 1020-1036

Emilia, D.A., Last, B.J. and Outhred, A.K. 1976. Gophysical exploration for groundwater in Ethiopia. Bull. Geophys. Obs. 16, 1-94.

Emilia, D.A.; Habte, G.C.; Dakin, F.M,; Fouchaux, R.E.; Outhred, A.K.; McCarthy, J. and Dante, W.M. 1975. Geophysical Groundwater exploration in Bati, Ethiopia, Bull. Geophys. Obs. 15, 107-117.

Getenet Mewa; Shimelis Fisseha; Dawit Mamo and Akalewold Seifu, 1996. Geophysical Studies for groundwater and dam site investigation in Raya Valley. Ethiop. Inst. Geol. Surv., Dept. Geophys, Addis Ababa pp

1-36. Dobrin, M.B. 1976. Introduction togeophysical prospecting (3rdedition). McGraw-Hill Book company, New York, pp.568-582.

Ghosh, D.P., 1971a. The application of linear filter theory to the direct interpretation of geoelectrical resistivity sounding measurements. Geophys. Prospect., V.19, p.192-217.

Grant, F.S. and West, G.F.1965. Interpretation theory in Applied Geophysics Mc Graw-Hill, New-York. 583 pp.

Habberjam, G.M. and Watkim, G.E., 1967. The reduction oflateral effects in resistivity plobing. Geophysics. prospect., V.15, p.221-235.

Hummel; J.N., 1932. A theoretical studyof apparent resistivityin survface potential methods. Trans, V.27, p.677-690.

Koefoed, O., 1979. Geosounding principles, 1, Resistivity sounding measurements. Elsevier, Amesterdam.

Koefoed,O., 1968. The application of the Kernell function in interpreting geoelectrical resistivity measurements. Gebrder Borntraeger, Berlin-Stuttgart.

Kramvis, S.C., 1987. Application of Electrical Resistivity in Ground water Exploration in cyprus. ph.D. thesis,Leicester Univ.

Keary, P. and Brooks, M., 1984. An Introduction toGeophysical Exploration. Black well Scientific publications, Oxford London Edinburgh.

Kazmin, V., 1975. Explanation of the Geological Map of Ethiopia. Ethiopian Institute of Geological surveys. Bulletin No. 1, oo. 1-14.

Keller, G.V. and Frischknecht, F.C. 1966. Electeical methods in geophysical prospecting, perogramon press, New York, pp. 519

Maillet,R., 1947. The fundamental equations of electrical prospecting. Geophysics, V.12, p.529-556.

Marseden, D., 1973. The automatic fitting of a resistivity sounding by geometric progression of depth. Geoph. prosp.21, 226-280.

Moges Tigabe, 1996. Geophysical Exploration of a Guried river valley for ground water in the Southern Borana Region Ethiop.Inst.Geol. Surv.Dept. Geophys, Addis Ababa, pp 1-5.

Mooney, H.M. and Wetzel, W.W., 1956. The potential about a point electrode and apparent resistivity curves for a two, three and four layered warth. the university of Mannesota press, Minneapolis.

Mundry,E., 1980. Short note on the effect of a finite distance potential electrodes on schlumberger resistivity, measurements--a simple correction gloph. Geophysics, V.45, pp.1872-1875.

Orellana, E. and Mooney, H.M., 1966. Master tables and curves for vertical electrical sounding over layered structures. Interciencia, Madid.

Parasnis, D.S. 1962, Prinsiples of applied geophysics (3rd edition). Chapman and Hall, London, pp. 98-121.

Pekeris, C.L., 1940. Direct method of interpretation in resistivity prospecting. Geophysics, V.S, pp.31-42.

Roy, A. and Apparao, A., 1971. Depth investigation in direct current methods: Geophysics, V.36, p.943-959.

Roy, K.K. and Elliot, H.M., 1951. Some observations regarding depth exploration in DC electrical methods. Geoexploration, V.19, p. 1-13

Slichter, L.B., 1933. The interpretation of the resistivity prospecting method for horizontal structures. Physics, v.4, p.307-322.

Telford, W.M.; Geldart, L.P. and Sheriff, R.E. 1976. Applied geophysics (4th edition). Cambridge University Press, Cambridge, pp. 677-686.

Tesfaye Chernet. 1993. Hydrogeology and Water resources development, EIGS, Addis Ababa, Ethiopia.

Van Overmeeren, R.A. 1981. A combination of electrical resistivity, Seismic Refraction and Gravity measurements for Groundwater exploration in the Sudan. Geophysics, 46,1304-13